

Dynamic Performance Analysis of Grid-Tied Hybrid Renewable Energy Systems under Fault Conditions: An IEEE 14-Bus system

Thomas Lukeyo^a, Cedric Okinda^{b,a,*}, Raymond Juma^a

^aDepartment of Electrical and Communications Engineering, School of Engineering and Built Environment, Masinde Muliro University of Science and Technology, Kakamega, Kenya.

^bCollege of Engineering, Laboratory of Modern Facility Agriculture Technology and Equipment Engineering of Jiangsu Province, Nanjing Agricultural University, Jiangsu 210031, P.R. China.

ABSTRACT

The global energy landscape is rapidly evolving towards increased reliance on renewable energy sources, driven by concerns over climate change and the finite nature of fossil fuels. However, the integration of variable and intermittent renewable energy sources into the electricity grid presents significant challenges to grid stability and reliability. This study presents a comparative analysis of Solar PV-Wind HRES Grid-Tied System and Solar PV-Wind-Battery HRES Grid-Tied System based on transient and steady-state stability analysis. The systems were simulated using the Electrical Transient Analyzer Program (ETAP®) and Grid-tied to an IEEE 14-bus system. For transient analysis, two common grid disturbances were explored, i.e., Line to Ground faults on buses and faults on the transmission line at different fault positions i.e., 0%, 10%, 25%, 50%, 75%, 90%, and 100% with a fault clearance time of 1.05 s, 1.50 s, and 2.00 s, and the fault set to occur at 1.00 s with a simulation time of 50 s. Lastly, ANOVA analysis was performed to analyze the effects of fault position on a transmission line, fault clearance time, and the presence of a battery energy system on the system settling time after a fault occurred based on generator speed, voltage, and frequency. For the Solar PV-Wind HRES Grid-Tied System, it was established that the voltage and frequency profiles at the Bus with the fault dropped significantly during the fault but recovered to their pre-fault level after the fault was cleared for all the explored fault clearance time. However, a larger fault clearance time (2.00 s) had a longer settling time. Furthermore, there were statistically significant differences between the explored fault clearance times. For the Solar PV-Wind-Battery HRES Grid-Tied System, it was established that the BESS enhanced the stability and efficiency of an HRES with voltages ranging from 0.98772 to 1.000 p.u. Moreover, there was a statistically significant interaction between the effects of fault clearance time and battery on the settling time for voltage, frequency, and generator speed. In comparison, the settling time for the Solar PV-Wind-Battery HRES Grid-Tied System was lower than that for the Solar PV-Wind HRES Grid-Tied System. Therefore, the battery energy system effectively compensates for the inherent variability of renewable energy sources preventing cascading failures and ensuring system robustness.

ARTICLE INFO

Keywords:

Grid-tied,
Renewable energy,
Transient stability,
Electrical Transient Analyzer Program,
Battery energy storage system.

Article History:

Received 11 October 2024
Received in revised form 15 December 2024
Accepted 17 December 2024
Available online 8 April 2025

1. Introduction

Currently, there has been an increase in the integration of large-scale renewable energy sources (RESs) in power systems due to climate change concerns, energy security, and sustainable development (IPCC, 2018; Medina et al., 2022; Newell et al., 2021). Among these RESs, Solar Photovoltaic (PV) and Wind energy conversion systems (WECS) have emerged as prominent contributors to the energy mix, owing to their availability, declining costs, and environmentally

friendly attributes (Hassan et al., 2024; IRENA, 2020; Kabeyi & Olanrewaju, 2022). Globally, renewable generation capacity reached 507 GW in 2023, with Solar PV and WECS accounting for about 96% (Celik, 2021). Additionally, the renewable generation capacity is projected to double by 2028 to about 710 GW (Mehra et al., 2021). However, the integration of these variable and intermittent RESs into the electricity grid presents significant challenges to grid stability and reliability

* Corresponding author. e-mail: cokinda@mmust.ac.ke.

Editor: [James Owuor](#), Masinde Muliro University of Science and Technology, Kenya.

Citation: Thomas, L., Cedric, O., & Raymond, J. (2024). Dynamic Performance Analysis of Grid-Tied Hybrid Renewable Energy Systems under Fault Conditions: An IEEE 14-Bus system. *Journal of Advances in Science, Engineering and Technology* 1 (2024), 1 – 24.

(Alam et al., 2020; Basit et al., 2020; Ourahou et al., 2020; Sinsel et al., 2020).

The stability of a power system is its ability to maintain synchronous operation and deliver power to consumers within acceptable voltage and frequency limits under steady-state and transient conditions (Flynn et al., 2019; Machowski et al., 2020; Shair et al., 2021). Transient stability relates to the system's ability to maintain synchronism following large disturbances such as faults, sudden changes in load, or the loss of generation (Khadka et al., 2020; Shair et al., 2021). On the other hand, steady-state stability concerns the long-term equilibrium of the system, ensuring that power flows remain balanced, and Voltage levels are within acceptable limits (Shair et al., 2021). Both transient and steady-state stability are essential for the reliable and efficient operation of power systems, including renewable energy integration (He et al., 2019). However, this study will focus on transient to analyze the system's ability to withstand and recover from disturbances.

Several factors contribute to the stability challenges faced by solar PV-wind Grid-tie hybrid renewable energy systems (HRESs) (Ahmed et al., 2024). Firstly, the inherent variability and unpredictability of solar and wind resources introduce fluctuations in power output, leading to V and f deviations in the grid (Ahmed et al., 2024; Bessa et al., 2019). Secondly, the dynamic behavior of power electronic converters used in hybrid system components, such as inverters and converters for energy storage devices, can influence system stability (Ahmed et al., 2024; Babu et al., 2020). Additionally, the interaction between renewable generation, energy storage, and grid-connected loads creates complex dynamic responses that require meticulous analysis and control (Pfeifer et al., 2018).

One of the early studies on transient stability in HRES was conducted by Bossanyi (2003), who explored the impact of wind power integration on the transient stability of power systems and highlighted that the intermittent nature of WECs could exacerbate stability issues, particularly during severe disturbances. However, Xu et al. (2019) indicated that the integration of RESs could improve the system's transient stability, provided that appropriate control mechanisms were in place. Nevertheless, regarding RES penetration levels, Alsakati et al. (2021) reported on a transient stability assessment of the IEEE 9-Bus system integrated wind power system and reported that high penetration and location of wind energy have a destabilizing impact on the power system.

More recent studies have focused on advanced control strategies to enhance the transient stability of HRES. Maaruf et al. (2022) proposed a robust sliding mode control strategy for both standalone and grid-connected operation of Solar-Wind-Battery HRES. The study reported a significantly improved robustness and better power management in terms of overshoot and settling time with enhanced tracking capability towards

the calculated optimal operation of the HRES under different external generation or load disturbances and internal parameter uncertainties. Additionally, Reza et al. (2023) and Venkatesan et al. (2024) investigated the use of coordinated control of battery energy storage systems (BESS) and flexible AC transmission systems (FACTS) devices in improving the transient stability of grid-tied HRES. The studies demonstrated that the coordinated control approach could effectively dampen oscillations and maintain synchronism during disturbances. Therefore, BESS plays a crucial role in system stability (Cifuentes et al., 2019; Farrokhbadi et al., 2017).

Current studies highlight several methods to enhance the stability of HRES. However, many studies focus on either solar PV or wind systems in isolation, without addressing the unique challenges posed by their combined operation in a grid-tied configuration (Emad et al., 2020). The integration of these hybrid systems into existing power grids requires advanced modeling and simulation tools to accurately predict and mitigate stability issues. Current simulations often lack the necessary detail and precision to capture the dynamic interactions between solar PV, wind turbines, and the grid, leading to potential oversights in stability analysis (Alnawafah, 2024). Therefore, developing robust models that can simulate the complex behavior of hybrid systems under various operating conditions is essential for ensuring their stable integration into the power grid. The main objective of the project is to examine the transient stability of a Grid-Tie solar PV-Wind HRES. With the specific objectives of developing a detailed and accurate IEEE 14 Bus system model for efficient integration of the solar PV-wind hybrid system. Analyzing the transient stability of the hybrid grid-tie system under sudden changes, i.e., faults on transmission lines and busses. Determining the impact of energy storage systems (BESS) on the stability and reliability of the grid-tied HRESs. The study will help understand the system's behavior under different operating conditions and identify strategies to enhance system stability.

2. Materials and Methods

This study aims to model, simulate, and analyze the impact of the integration of RESs on the transient stability of the grid using Electrical Transient Analyzer Program (ETAP®) simulation software. For a comparative analysis, the study evaluated both Solar PV-Wind and Solar PV-Wind-Battery HRESs regarding the settling time (t_s) for generator speed (G_s), voltages (V), and frequency (f) under sudden changes, i.e., faults on transmission lines and busses (Note that all transmission lines and buses were faulted and analyzed in this study) under varying fault clearance time (t_{ct}). Additionally, the study examined the impact of the fault position (F_p), on the transmission line by varying the position of the fault on a transmission line along its length. The research design flow for this introduced study is given in Fig. 1. Furthermore, Transient stability focuses on the system's ability to maintain synchronism when subjected to large disturbances, thus, Line-to-ground (LG) fault was

applied. The choice for LG was because it's the most common type of system fault in power systems (Datta et al., 2020).

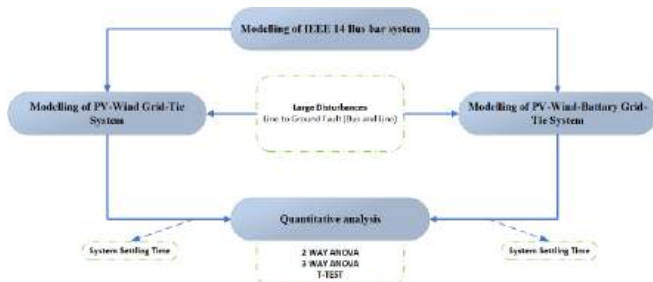


Fig. 1: The research design flow

2.1. Simulation of IEEE 14-bus System

The simulation of the IEEE 14-bus system using ETAP® provided an in-depth analysis of power flow and stability within a standard test case for electrical power systems. The IEEE 14-bus system, a simplified model representing a portion of the American Electric Power

(AEP) system (Midwestern U.S.), is widely used in academic and industry research for validating algorithms and methodologies in power system analysis (Do Coutto Filho et al., 2022). The IEEE 14-bus system was modeled to include 14 buses, 5 generators, 14 loads, 17 transmission lines, and 4 transformers (Reddy et al., 2016). The data used in modeling the IEEE 14-bus system is given in Table 1.

The modeling and simulation process began with the drawing of the one-line diagram of the system after which power flow analysis was performed, i.e., Load Flow Analysis based on the Newton- Raphson method (Akram & Ann, 2015) which calculates the V magnitudes and angles at each bus, as well as the power flowing through the transmission lines. This analysis helped to identify areas of potential V instability, power losses, and bottlenecks in the system before the addition of Solar PV and WECs (stable buses far from the generators, Solar PVs, WECs, and BESSs resources were added).

Table 1: The Simulated Solar PV-Wind grid tied System data

Wind Turbine					
Wind turbine	MW		kV		PF
WTG2_13-2	20		0.575		95
WTG2_10-2	20		0.575		95
Solar PVs					
Solar PV	Cells	V(DC)	Panels		kW (DC)
PV A3_3-2	60	1000	400		91.71
PV A1_14-2	60	1000	500		113.1
Inverters					
Inverter	kW (DC)	V (DC)	KVA (AC)		kV (AC)
Inv1	166.7	33	150		33
Inv2	200	33	180		33
Batteries					
Battery	Strings	Plates	Cells		Capacity (AH)
Battery_1	1	37	250		1350
Battery_2	1	37	250		1350
Charger inverter					
	KVA (AC)	KV (AC)	PF	KW (DC)	V (DC)
Charger_1	5	33	85	3.83	600
Charger_2	5	33	85	3.83	600
Inv_1	225	33	99	250	600
Inv_2	135	33	99	150	600

2.2. Data collection

The ETAP® simulation facilitates transient stability of the HRES grid-tie system. Two plausible grid disturbances were explored, i.e., faults on buses and faults on the transmission line at varying F_p (0%, 10%, 25%, 50%, 75%, 90%, and 100%). For both disturbances, the faults' occurring time was set to 1.0 s while the t_{ct} was varied incrementally, i.e., 1.05 s, 1.5 s, and 2.0 s. The transient stability analysis in ETAP® assesses the system's response to these disturbances through the analysis of the t_s . This is a time-domain simulation that involves solving the differential-algebraic equations (DAEs) that govern the system's dynamics over a short period, typically ranging from a few milliseconds to several seconds, therefore, the simulation time was set to 50.0 s in this study.

Transient stability data was collected through the following steps. Firstly, LG fault was simulated on each bus, and the t_s for G_s (for all generators), V (for all

buses), and f (for all buses) were collected for each t_{ct} . Secondly, LG fault was simulated on each transmission line at different F_p , for each F_p the t_s for G_s (for all generators), V (for all buses), and f (for all buses) were collected for each t_{ct} . Lastly, the role of the energy storage system in enhancing transient stability was analyzed. All the t_s was collected via the Excel data export option in ETAP and saved in the internal storage of Microsoft Windows 11 PC (intel core i5-iRISXe CPU, 4 GHz, 16 GB (Intel, Santa Clara, CA, USA)).

2.3. Statistical analysis

This study aimed to analyze stability based on t_s for Solar PV-Wind HRES and Solar PV-Wind-Battery HRES and provide a comparative analysis. All statistical computations were performed using SPSS software package version 25.0 (SPSS Inc., Chicago, IL, USA). Before the statistical analysis, the data was tested for normality using the Shapiro-Wilk Test of Normality (González-Estrada et al., 2022) to guide the choice for .

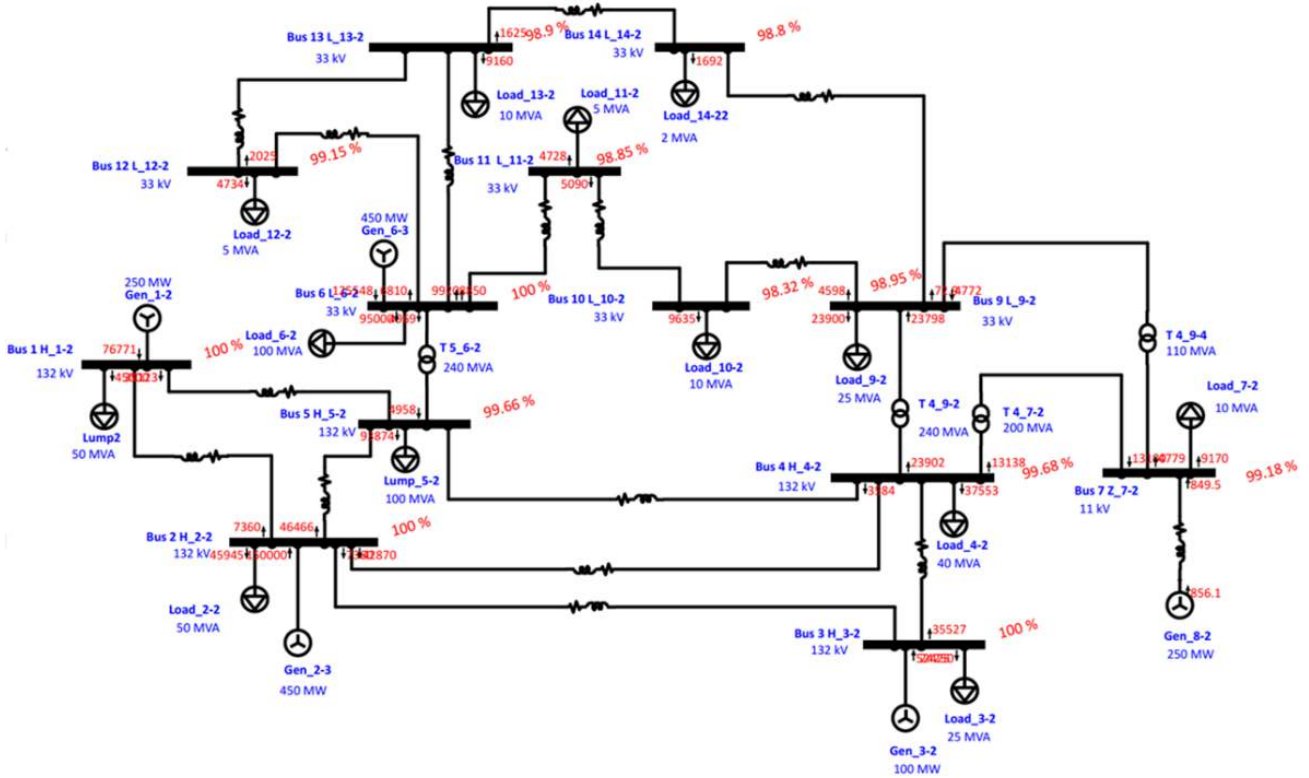


Fig. 2: The simulated IEEE 14-bus system and Load Flow Analysis

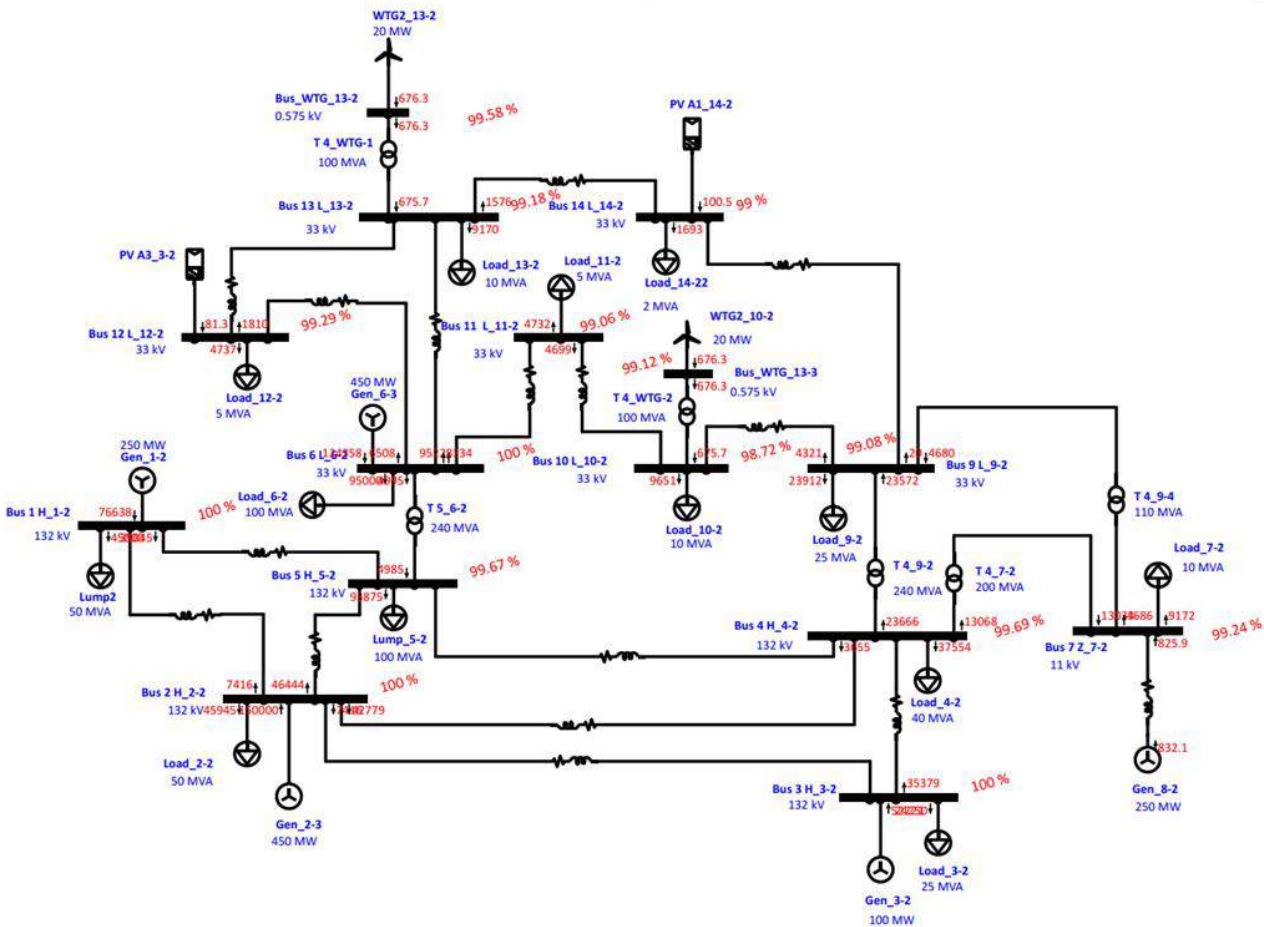


Fig. 3: The simulated Solar PV-Wind HRES Grid-Tied System and Load Flow Analysis

parametric or non-parametric analysis as well as data transformation to achieve normality. This study was

divided into two sections, firstly, for a Grid-Tied Solar PV-Wind HRES the aim was to examine the effect of t_{ct} ,

and F_p on the t_s , therefore 2-way ANOVA (Sommerfield et al., 2021a) was applied. Secondly, 3-way ANOVA (Sommerfield et al., 2021b) was applied to determine the effect of t_{ct} , F_p and Battery on the t_s of a Grid-Tied Solar PV-Wind-Battery HRES. Additionally, a T-Test (De Winter, 2019) was performed to establish if there was a statistically significant difference between t_s of a Grid-Tied Solar PV-Wind HRES and t_s of a Grid-Tied Solar PV-Wind-Battery HRES.

3. Results and Discussions

3.1. IEEE 14BUS system evaluation

The simulation of the IEEE 14-bus system using ETAP software provided valuable insights into the operational performance and stability characteristics of a typical power system network under various scenarios. The simulated IEEE 14-bus system is given in Fig. 2.

The load flow analysis was conducted to determine the steady-state operating conditions of the IEEE 14-bus system. The simulation results revealed the V levels at each bus, the power flows along transmission lines, and the power losses in the network. The results indicated that the system operated within acceptable V limits, with bus V ranging between 0.98 p.u. and 1.00 p.u. The power losses were also minimal, highlighting the efficiency of the network under normal operating conditions. The bus with the lowest bus V was Bus 10 (0.9832 p.u.) while Bus 1, 2, and 3 had the highest bus voltage of 1.00 p.u. This is attributed to the busses being directly connected to the generator which provides a stable power supply and minimizes the potential for V fluctuations as also presented by the study by Hamzeh et al. (2018).

The objective of this study was to evaluate the transient stability of the Solar PV-Wind HRES Grid-Tie System, therefore, stability analysis wasn't conducted for the IEEE 14-bus System. However, several studies have been performed on the stability analysis for the IEEE 14-bus System (Hashim et al., 2012; Iyambo & Tzoneva, 2007; Kumar et al., 2020; Siva et al., 2020) under different system faults and simulation software

The Load Flow (Power Flow) analysis is a fundamental step in power system studies, especially when integrating renewable energy sources like Solar PV and WEC resources. The primary goal of this analysis was to identify the most suitable candidate buses for incorporating these RESs into the grid. The criteria for selection focused on buses that were furthest from the generator but maintained a stable voltage profile, ensuring that the integration of RESs would enhance grid stability rather than compromise it i.e., Bus 10 for wind, Bus 12 for Solar PV, Bus 13 for wind, and Bus 14 for Solar PV as presented in Fig. 3. In power systems, the distance of a bus from the generator can significantly influence V stability (Hosseinzadeh et al., 2021). Buses that are further from the generator often experience more significant V drops due to the increased impedance of the transmission lines (Hosseinzadeh et al., 2021; Petinrin & Shaabanb, 2016). However, if a bus far from

the generator maintains a stable voltage, it suggests that the system at that location is resilient and can handle additional loads or generation without compromising overall stability (Blaabjerg et al., 2017; Hosseinzadeh et al., 2021; Ismail et al., 2020). Therefore, these buses are prime candidates for the integration of distributed generation sources such as Solar PVs and WECs.

3.2. Solar PV-Wind HRES Grid-Tied System

The solar PV system was connected to Bus 12 (PV A3_3-2) and 14 (PV A1_14-2) as presented in Fig. 3. The PV system was modeled with an inverter-based interface, equipped with a Maximum Power Point Tracking (MPPT) controller to optimize power output under varying solar irradiance conditions. Two WECs were connected to Bus 10 (WTG2_13-2) and 13 (WTG2_10-2), each via a 100 MVA step-up transformer. Detailed specifications of the modeled components are given in Table 1. The wind turbine model included a variable-speed wind turbine coupled with a doubly-fed induction generator (DFIG). The control system for the wind turbine was modeled to regulate rotor speed and maintain grid stability during wind speed fluctuations.

The load flow analysis was conducted to establish the operating conditions of the IEEE 14-bus system with the integrated HRES. The following were established: Firstly, the voltages at all buses were maintained within acceptable limits (Fig. 3), with slight variations observed at buses connected to the Solar PV and WECs resources due to their intermittent nature. The voltage at Bus 12 and 14 (connected to the PV system) was 0.9929 p.u. and 0.9999 p.u., respectively. While the voltage at Bus 10 and 13 (connected to the WEC) were 0.9878 p.u. and 0.9918 p.u., respectively. These slight variations in voltage are attributable to the intermittent nature of the PV and wind systems, which can cause fluctuations in power output depending on irradiation and wind speed environmental conditions (Shivashankar et al., 2016). These results are consistent with a study by Benali et al. (2018) who reported that V stability can be achieved by PV and Wind connected to the same point of common coupling (PCC) with a sensitive load. Similarly, Ahmed et al. (2020) discussed that integrating large Solar PV and WECs can improve the V profile of a power system. This is because these RESs can provide additional reactive power support, which helps in maintaining voltage levels within the desired range.

Secondly, the integration of Solar PVs and WECs systems into the IEEE 14-bus system also resulted in noticeable changes in power flow patterns, particularly on the lines connected to Buses 10, 11, 12, 13, and 14. The power flows on these lines increased due to the additional generation from RESs but remained within the thermal limits of the transmission lines (Basit et al., 2020). These changes are significant because they can affect the overall load distribution and efficiency of the power system (Das et al., 2018). The power flows on these lines may increase or decrease depending on the generation from the PVs and WECs systems at any given time, which can lead to congestion in some lines or under-utilization of others (Samakpong et al., 2022).

Managing these power flows is essential for optimizing the performance of the grid and ensuring that it can handle the variable nature of RESs (Abdi et al., 2017; Panda & Das, 2021; Reddy, 2017).

Lastly, the integration of RESs, specifically in HRES has been found to result in a slight increase in total system losses, averaging around 0.02%. This phenomenon is primarily attributed to the additional reactive power flows introduced by the integration of RESs such as solar PVs and WECs systems. Reactive power, which does not perform useful work, can lead to increased losses in the system, as highlighted by (Yang et al., 2017). However, this increase is considered marginal, signifying that the overall system efficiency remains largely unaffected (Li et al., 2016). The minimal impact on system efficiency is crucial for the broader adoption of HRES (Babatunde et al., 2020). As the world moves towards sustainable energy solutions, concerns about the efficiency and reliability of these systems are paramount. The review by Roy et al. (2022) suggests that despite the slight increase in losses, the integration of HRES does not significantly compromise the system's performance. This outcome is particularly significant in the context of grid-tied systems, where maintaining high efficiency is critical to ensuring the reliability and stability of the entire power network (Shair et al., 2021; Shakerighadi

et al., 2023). Moreover, the slight increase in losses can be managed and mitigated through advanced control strategies and optimization techniques (Sarkar et al., 2018).

The impact of these losses can be further minimized, enhancing the overall performance of the system by fine-tuning the reactive power management and employing sophisticated grid management tools (Kow et al., 2016). This aligns with the ongoing research and development in the field of renewable energy, where the focus is not only on maximizing energy generation but also on optimizing system performance to ensure sustainability and efficiency (Abdmouleh et al., 2017; Amran & Muhtazaruddin, 2019; Østergaard et al., 2020; Potřč et al., 2021).

3.3. Transient stability evaluation

The transient stability analysis focused on the system's response to severe disturbances, i.e., LG at all buses and lines. The t_s and system responses were analyzed in detail. Note that the t_s is the time it takes for a response to stabilize within a small percentage (usually 5% or 2%) of its final value. For this study, the tolerance band was set to 2% to improve performance, and accuracy and reduce variability (Corneo & Jeanne, 2009).

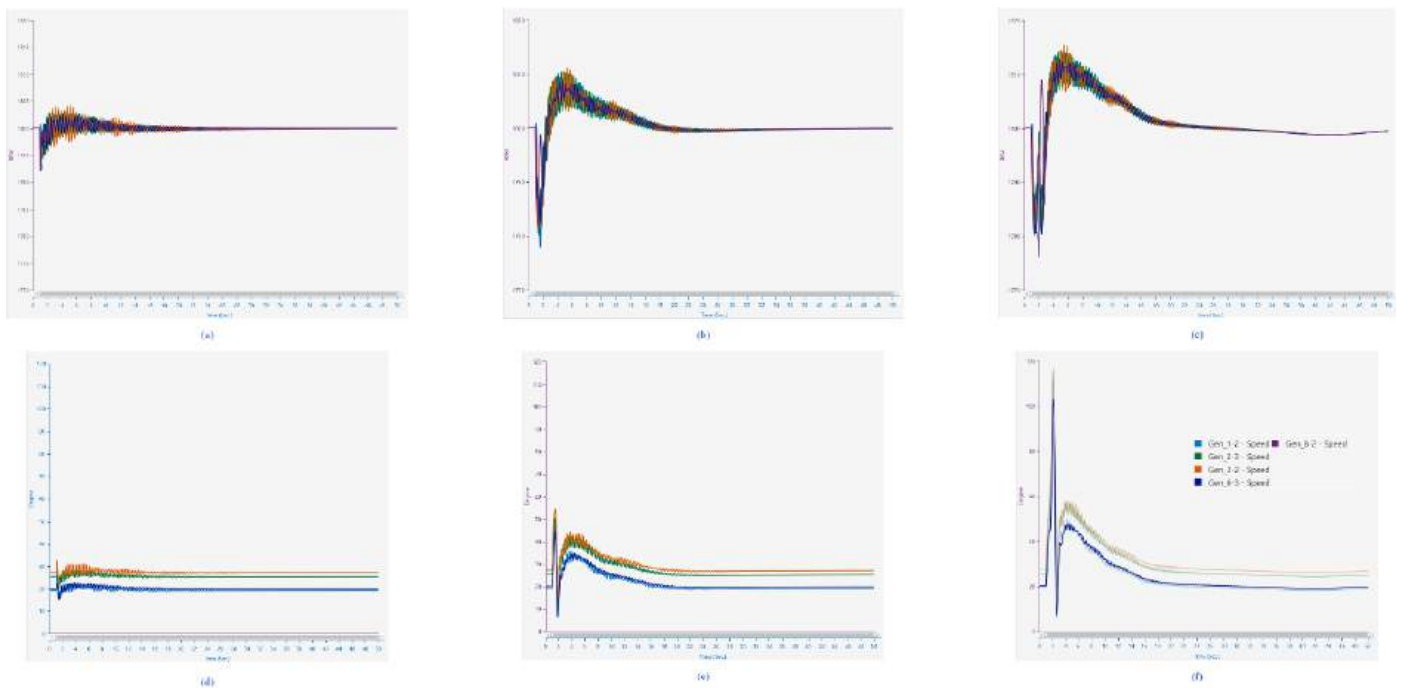


Fig. 4: The plots for Power angle and Speed for the synchronous generators with a fault on Bus 1, (a) Speed at $t_{ct} = 1.05$ s, (b) Speed at $t_{ct} = 1.50$ s, (c) Speed at $t_{ct} = 2.00$ s, (d) Power angle at $t_{ct} = 1.05$ s, (e) Power angle at $t_{ct} = 1.50$ s, (f) Power angle at $t_{ct} = 2.00$ s.

3.3.1. Fault on buses

An LG fault was simulated on all the buses (one at a time) at 1.0 s and t_{ct} at 1.05 s, 1.5 s, and 2.0 s. Fig. 4 presents the plots for the power angles and generator speeds against time when the LG fault was simulated in Bus 1. Generally, the synchronous generators in the system exhibited significant oscillations immediately after the fault. However, the system remained stable as

the oscillations dampened. Additionally, the t_s was directly proportional to the t_{ct} .

The response of synchronous generators to faults is critical in determining the overall stability of the system. The observation that the synchronous generators in the system exhibited significant oscillations immediately after the fault is consistent with typical transient responses in power systems (Xiong et al.,

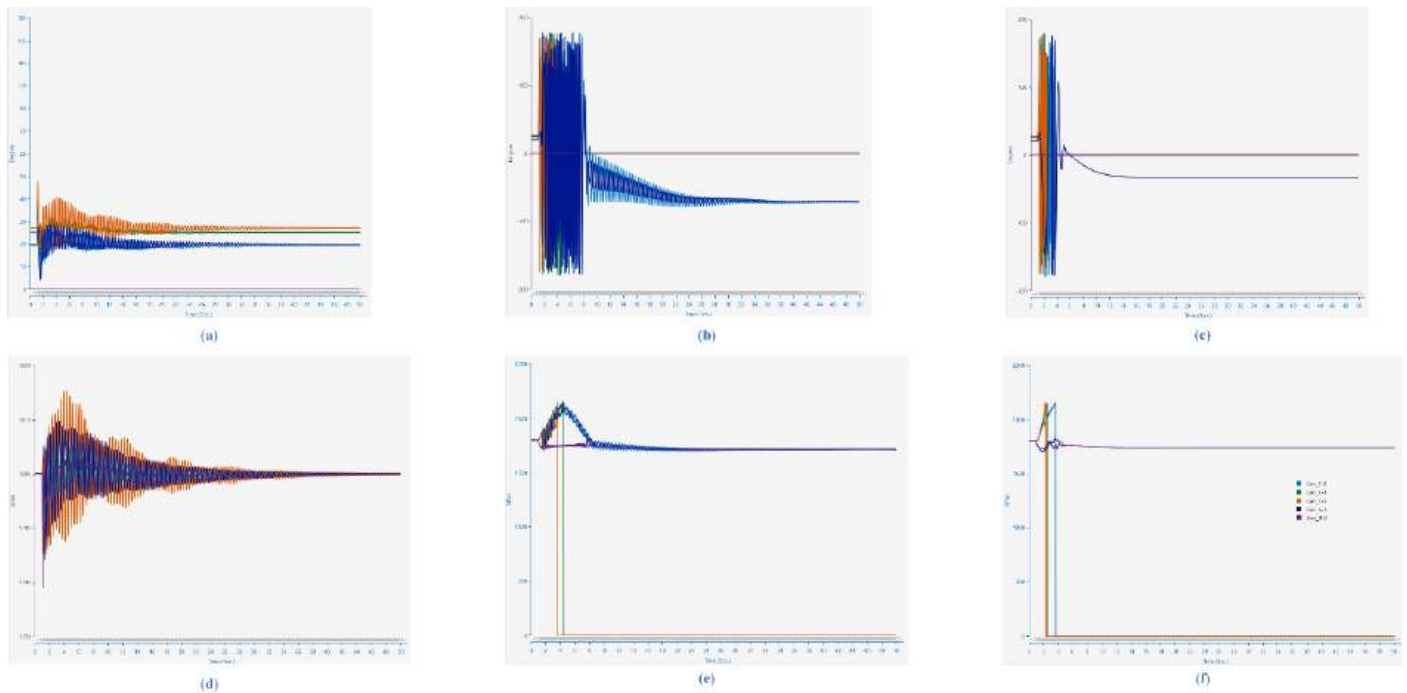


Fig. 6: The plots for Power angle and Speed for the synchronous generators with a fault on transmission Line 1 at 50% fault position, (a) Power angle at $t_{ct} = 1.05$ s, (b) Power angle at $t_{ct} = 1.50$ s, (c) Power angle at $t_{ct} = 2.00$ s, (d) Speed at $t_{ct} = 1.05$ s, (e) Speed at $t_{ct} = 1.50$ s, (f) Speed at $t_{ct} = 2.00$ s

the fault persists, the more severe the V and f deviations, which can pose serious challenges to grid stability and reliability.

The relationship between t_{ct} and the severity of V and f drops can be explained by the delayed response of the RESs in injecting reactive power (Basit et al., 2020; Milo et al., 2021; Stanelytė & Radziukynas, 2022). Therefore, when the fault is cleared quickly, RESs can respond almost immediately, minimizing the impact on the grid (Basit et al., 2020). Conversely, a delayed clearance means that the system operates under fault conditions for a longer period, leading to more significant disruptions before stabilization efforts can take effect (Morshed & Fekih, 2019).

3.3.2. Fault on Transmission Lines

Similarly, an LG fault was simulated on all the transmission lines (one at a time) at 1.0 s and the fault was cleared at varied t_{ct} of 1.05 s, 1.5 s, and 2.0 s. Additionally, in the simulation the F_p was varied at intervals from 0% to 100% of the line length. Fig. 6 presents the plots for the power angles and generator speeds against time at a F_p of 50%. It can be observed that at a t_{ct} of 1.05 s, the oscillations within the system are sufficiently dampened, allowing the generators to regain stability. This implies that a timely clearance of faults is critical for maintaining the operational stability of the system (Nsaif et al., 2021). Specifically, when faults are cleared within this time frame, the system's transient stability is preserved (James et al., 2017), and the oscillatory behavior of the power angles is mitigated, leading to a steady-state condition where the generators can continue functioning without being isolated from the

grid (Meegahapola et al., 2020). However, when the t_{ct} is extended beyond 1.05 seconds, a different dynamic unfolds. As depicted in Fig. 6 (e) and (f), generators connected to the faulted line are eventually isolated from the system (Nagpal & Henville, 2017). This isolation occurs because the extended presence of the fault leads to more pronounced oscillations in the system, making it difficult for the generators to maintain synchrony with the rest of the grid (Auer et al., 2017). The instability is further evidenced by the power angle oscillations, which begin to swing between positive and negative values, as shown in Fig. 6 (b) and (c). These oscillations indicate a loss of synchronism, which is a precursor to the generators being disconnected from the network to prevent further damage or instability in the broader system (Sharafutdinov et al., 2018).

The effect of F_p and t_{ct} was also analyzed to determine the effect of the F_p and t_{ct} on system stability based on f and V . From the Fig. 7 and Fig. 8, it can be observed that F_p doesn't have much effect on the f and V profiles. Therefore, the location of the fault on a transmission line does not significantly alter the system's f and V characteristics (Chen et al., 2016; Chen et al., 2017).

However, the t_{ct} had a noticeable effect. i.e., the t_s of 1.50 s and 2.00 s were longer compared to those of 1.05 s. This indicates that the duration it takes to clear a fault is crucial in determining the system's ability to return to stable f and V levels. The increased t_s associated with longer fault clearance intervals suggest that delays in clearing faults can exacerbate instability and prolong the recovery process (Wang et al., 2016).

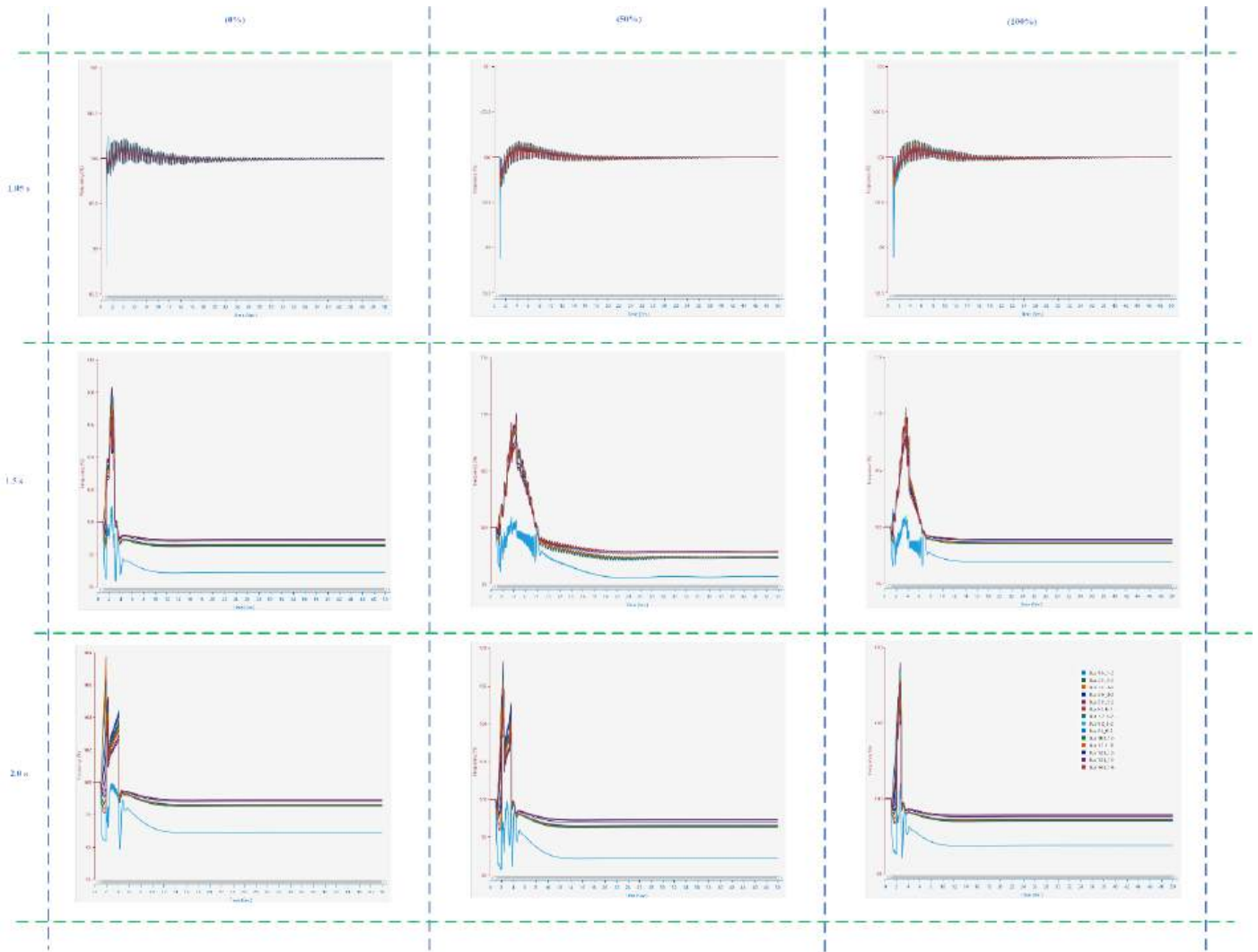


Fig. 7: The plots for Frequency at different F_p and t_{ct}

3.4. Quantitative analysis

A descriptive statistic of the entire data is given in Table 2 in terms of measures of central tendency and measures of variability (spread) in t_s for G_s , V , and f . It was established that the mean t_s for G_s was 15.843 s with a median of 6.596 s ranging from 1.021 s (minimum) to 50.000 s (maximum). The mean t_s for f was 8.898 s with a median of 5.991 s ranging from 1.050 s (minimum) to 49.981 s (maximum). Lastly, the mean t_s for V was 14.810 s with a median of 5.551 s ranging from 1.021 s (minimum) to 50.000 s (maximum).

The Shapiro-Wilk Test of Normality revealed that the initial dataset was not normally distributed, which is crucial because many statistical analyses assume normality to yield valid results (Shapiro & Wilk, 1965). The test's outcome indicates a deviation from the normal distribution, as further evidenced by the positive skewness reported in Table 2. A positively skewed distribution suggests that the data has a longer tail on the right side, meaning that higher values are more spread out (Rousselet & Wilcox, 2018). Therefore, a logarithmic (Log) transformation was applied to the data (Lee, 2020).

Table 2: The descriptive statistics of the setting time for generator speed bus frequency and bus voltage (n = 4060).

Descriptive statistics	Speed (s)	Frequency (s)	Voltage (s)
Maximum	50.000	1.050	50.000
Minimum	1.021	49.981	1.021
Range	48.9794	48.931	48.979
Interquartile Range	19.030	9.170	17.010
Median	6.596	5.991	5.551
Skewness	1.083	2.237	1.282
Mean	15.843	8.898	14.810
Standard error	0.283	0.168	0.268
Standard deviation	18.050	10.732	17.052
Variance	325.807	115.168	290.776

3.4.1. Fault on buses

For each variable, i.e., f , V , and G_s , the t_s was analyzed as presented in Table 3. Firstly, a one-way ANOVA was conducted to examine the effect of t_{ct} on t_s of a Solar-PV-Wind HRES Grid-tied to an IEEE 14 bus system based on V . It was established that there was a statistically significant difference between $t_{ct} = 1.05 s$, $t_{ct} = 1.50 s$, and $t_{ct} = 2.00 s$ groups ($p < 0.05$). A Tukey post hoc test revealed that t_s was statistically

significantly lowest for $t_{ct} = 1.05 s$ and highest for $t_{ct} = 2.00 s$ ($p < 0.05$). These results ascertain that a shorter t_{ct} leads to faster V stabilization, which could be indicative of a more robust system response to disturbances. However, there was no statistically significant difference between the $t_{ct} = 1.50 s$, and $t_{ct} = 2.00 s$ groups. This implies that after a certain threshold, increasing t_{ct} does not further delay the system's V response significantly.

Table 3: The statistical results of the settling time (t_s) expressed in terms of mean and standard deviation

Fault clearance time (t_{ct})	f (t_s)	V (t_s)	G_s (t_s)
$t_{ct} = 1.05 s$	5.316 ± 0.448^a	10.696 ± 0.587^a	11.108 ± 0.549^a
$t_{ct} = 1.50 s$	7.379 ± 0.491^b	12.526 ± 0.404^b	14.256 ± 0.605^b
$t_{ct} = 2.00 s$	9.315 ± 0.509^b	12.438 ± 0.591^b	15.005 ± 0.628^b

a, b mean \pm std within a column with no superscript in common differ significantly ($p < 0.05$)

Secondly, a one-way ANOVA was conducted that examined the effect of t_{ct} on t_s of a Solar-PV-Wind HRES Grid-tied to an IEEE 14 bus system based on f . Similarly, it was established that there was a statistically significant difference between $t_{ct} = 1.05 s$, $t_{ct} = 1.50 s$, and $t_{ct} = 2.00 s$ groups ($p < 0.05$). A Tukey post hoc test revealed that t_s was statistically significantly lowest for $t_{ct} = 1.05 s$ and highest for $t_{ct} = 2.00 s$ ($p < 0.05$). However, there was no statistically significant

difference between the $t_{ct} = 1.50 s$, and $t_{ct} = 2.00 s$ groups. The lack of a significant difference between the 1.50 s and 2.00 s t_{ct} groups suggest a plateau in the impact of t_{ct} on frequency stabilization beyond a certain point. The observed trend across both V and f analyses indicates that a shorter critical clearing time is generally associated with quicker system stabilization, which is crucial in maintaining grid reliability and preventing cascading failures (Guo et al., 2017).

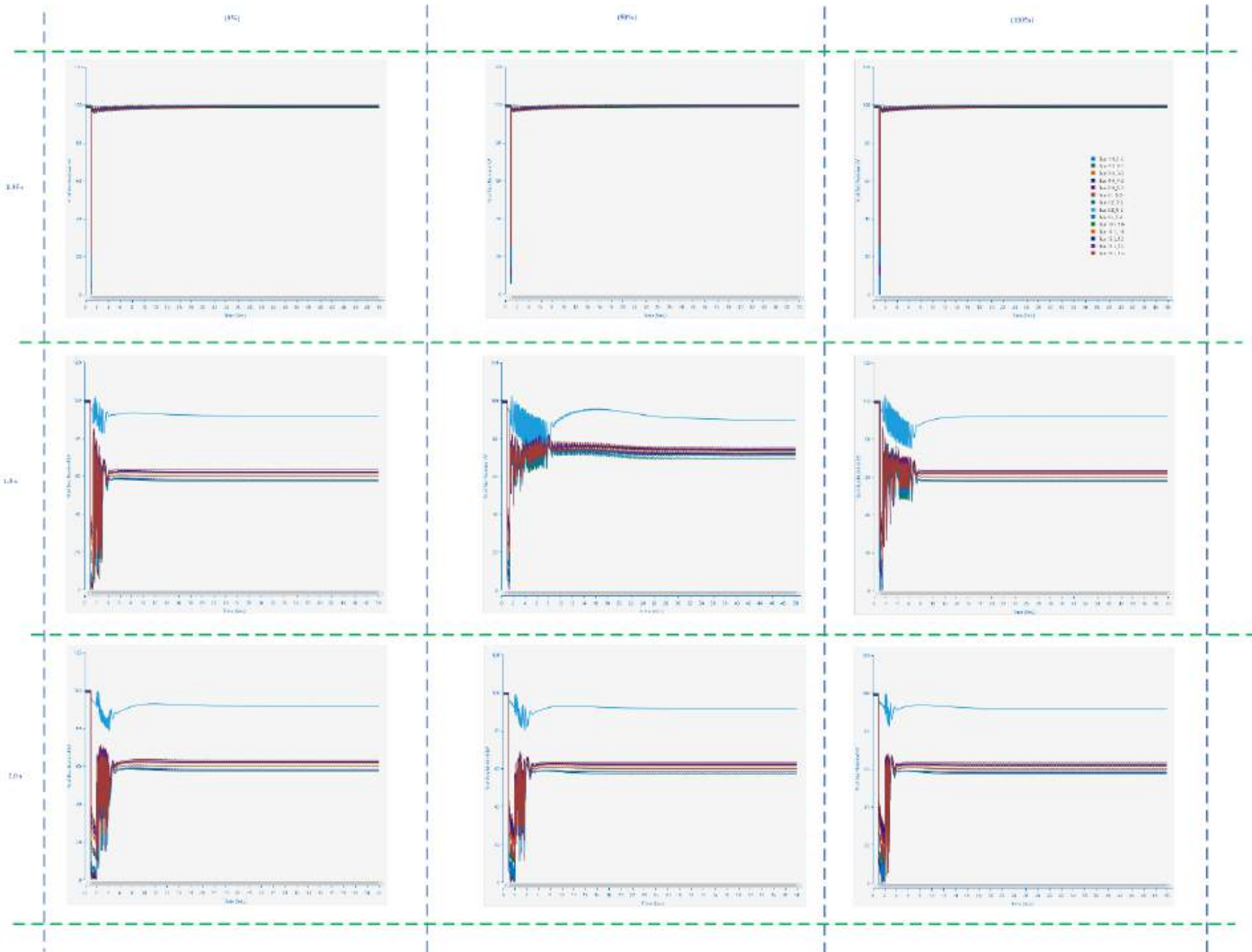


Fig. 8: The plots for Voltage at different F_p and t_{ct}

Lastly, a one-way ANOVA was conducted that examined the effect of t_{ct} on t_s of a Solar-PV-Wind HRES Grid-tied to an IEEE 14 bus system based on G_s . Similarly, it was established that there was a statistically significant difference between $t_{ct} = 1.05 s, t_{ct} = 1.50 s$, and $t_{ct} = 2.00 s$ groups ($p < 0.05$). A Tukey post hoc test revealed that t_s was statistically significantly lowest for $t_{ct} = 1.05 s$ and highest for $t_{ct} = 2.00 s$ ($p < 0.05$). However, there was no statistically significant difference between the $t_{ct} = 1.50 s$, and $t_{ct} = 2.00 s$ groups. Generally, this consistent pattern across all the analyzed stability parameters underscores the critical role of t_{ct} in determining the dynamic performance of the HRES. The $f, V, \text{ and } G_s$, shows that shorter t_{ct} are beneficial for system stability, as they reduce the duration of disturbances and allow the system to return to steady-state operation more rapidly.

The results of these analyses indicate a clear relationship between t_{ct} and the stabilization times of $f, V, \text{ and } G_s$ in a Solar-PV-Wind HRES grid tied to an IEEE 14 bus system. Across all three parameters, shorter t_{ct} values consistently led to faster stabilization times, which is advantageous for maintaining system stability during transient disturbances. The lack of significant differences between $t_{ct} = 1.50 s$, and $t_{ct} = 2.00 s$ suggests that while extending t_{ct} beyond 1.50 s may not yield further benefits in stabilization time, reducing t_{ct} below this threshold is critical for optimal system

performance. These findings highlight the importance of carefully selecting t_{ct} to ensure both the reliability and efficiency of hybrid renewable energy systems connected to the grid.

3.4.2. Fault on Transmission Lines

As already mentioned, the fault on the transmission line was varied at different F_p as the fault was cleared at varying t_{ct} a summary of the data is given in Table 4. For each variable, i.e., $f, V, \text{ and } G_s$, the t_s was analyzed as presented in Table 6.

Firstly, a two-way ANOVA was conducted that examined the effect of t_{ct} and F_p on t_s of a Solar-PV-Wind HRES Grid-tied to an IEEE 14 bus system based on V . There was a statistically significant interaction between the effects of t_{ct} and F_p on the t_s of V ($p < 0.05$). thus, the combined effect of t_{ct} and F_p on the t_s of V is more complex than the individual effects of these factors. However, there was no statistically significant difference in the F_p on the t_s of V ($p < 0.05$). Indicating that variations in F_p do not independently influence the V stability significantly. Additionally, there was a statistically significant difference in the t_{ct} on the t_s of V ($p < 0.05$), with $t_{ct} = 2.00 s$ having a significantly higher t_s than all the other t_{ct} . Therefore, a longer t_{ct} could lead to more extended periods before V stability is re-established after a disturbance.

Table 4: A summary of the data on the effect of fault position (F_p) and fault clearance time (t_{ct}) on settling time (t_s) for Frequency (f), voltage (V), and generator speed (G_s).

F_p	t_{ct}	f (t_s)	V (t_s)	G_s (t_s)
0% mean \pm std	$t_{ct} = 1.05 s$	2.608 \pm 0.253	1.381 \pm 0.138	1.841 \pm 0.218
	$t_{ct} = 1.50 s$	11.545 \pm 0.261	7.687 \pm 0.193	11.738 \pm 0.306
	$t_{ct} = 2.00 s$	24.575 \pm 0.436	12.296 \pm 0.472	27.853 \pm 0.524
10% mean \pm std	$t_{ct} = 1.05 s$	2.522 \pm 0.245	1.489 \pm 0.137	1.813 \pm 0.204
	$t_{ct} = 1.50 s$	14.459 \pm 0.330	9.235 \pm 0.175	16.132 \pm 0.356
	$t_{ct} = 2.00 s$	33.709 \pm 0.482	18.629 \pm 0.440	34.360 \pm 0.482
25% mean \pm std	$t_{ct} = 1.05 s$	2.657 \pm 0.259	1.496 \pm 0.147	1.768 \pm 0.197
	$t_{ct} = 1.50 s$	17.027 \pm 0.283	10.421 \pm 0.246	18.801 \pm 0.398
	$t_{ct} = 2.00 s$	25.226 \pm 0.465	21.407 \pm 0.441	30.560 \pm 0.455
50% mean \pm std	$t_{ct} = 1.05 s$	2.394 \pm 0.229	1.560 \pm 0.150	1.832 \pm 0.199
	$t_{ct} = 1.50 s$	12.170 \pm 0.287	8.5168 \pm 0.127	12.704 \pm 0.297
	$t_{ct} = 2.00 s$	31.419 \pm 0.458	16.619 \pm 0.495	32.010 \pm 0.502
75% mean \pm std	$t_{ct} = 1.05 s$	2.430 \pm 0.239	1.545 \pm 0.147	1.662 \pm 0.179
	$t_{ct} = 1.50 s$	11.987 \pm 0.279	7.435 \pm 0.166	12.216 \pm 0.300
	$t_{ct} = 2.00 s$	30.620 \pm 0.456	14.874 \pm 0.549	31.338 \pm 0.534
90% mean \pm std	$t_{ct} = 1.05 s$	2.728 \pm 0.243	1.617 \pm 0.160	1.958 \pm 0.211
	$t_{ct} = 1.50 s$	12.388 \pm 0.286	8.414 \pm 0.158	13.017 \pm 0.291
	$t_{ct} = 2.00 s$	28.761 \pm 0.508	17.772 \pm 0.587	33.626 \pm 0.554
100% mean \pm std	$t_{ct} = 1.05 s$	2.964 \pm 0.262	1.519 \pm 0.165	2.170 \pm 0.246
	$t_{ct} = 1.50 s$	10.639 \pm 0.275	8.196 \pm 0.180	11.252 \pm 0.283
	$t_{ct} = 2.00 s$	29.020 \pm 0.497	14.490 \pm 0.551	33.981 \pm 0.538

Secondly, a two-way ANOVA was conducted that examined the effect of t_{ct} and F_p on the t_s of a Solar-PV-Wind HRES Grid-tied to an IEEE 14 bus system based on f . There was a statistically significant interaction between the effects of t_{ct} and F_p on the t_s of f ($p < 0.05$). This indicates that the interaction between these factors critically affects how quickly the system f stabilizes after a disturbance. A simple main effects analysis showed that $t_{ct} = 2.00 s$ had a significantly higher t_s than $t_{ct} = 1.05 s$ and $t_{ct} = 1.50 s$ for all F_p . This finding reinforces the notion that larger t_{ct} are

associated with delayed stabilization across different F_p levels. Additionally, there were statistically significant differences between F_p 1 (0%) and F_p 2 (10%), F_p 3 (25%), F_p 4 (50%), and F_p 6 (90%), between F_p 2(10%) and F_p 7 (100%), between F_p 3(25%) and F_p 5 (75%) and F_p 6 (90%), between F_p 7(100%) and F_p 3 (25%) and 4 (50%) on the t_s of f ($p < 0.05$). These differences highlight the influence of F_p levels on f stability, suggesting that as the F_p level increases, the time required for the f to settle also changes, although the relationship is not strictly linear.

Table 5: The statistical results of the settling time (t_s) expressed in terms of mean and standard deviation

Fault position (F_p)	$f(t_s)$	$V(t_s)$	$G_s(t_s)$
0% mean \pm std	7.121 \pm 0.468 ^g	12.909 \pm 0.491	13.811 \pm 0.572 ^a
10% mean \pm std	9.577 \pm 0.502 ^{d^{ef}}	16.097 \pm 0.557	17.043 \pm 0.617 ^b
25% mean \pm std	11.108 \pm 0.530 ^d	14.991 \pm 0.531	17.069 \pm 0.610 ^b
50% mean \pm std	9.092 \pm 0.488 ^{ad}	15.641 \pm 0.536	15.633 \pm 0.586 ^b
75% mean \pm std	8.092 \pm 0.478 ^{bc^{eg}}	15.317 \pm 0.533	15.375 \pm 0.598 ^b
90% mean \pm std	9.268 \pm 0.506 ^{ac^f}	14.626 \pm 0.516	16.200 \pm 0.594 ^b
100% mean \pm std	8.068 \pm 0.494 ^{bc^g}	14.208 \pm 0.503	15.801 \pm 0.583 ^b

a, b mean \pm std within a column with no superscript in common differ significantly ($p < 0.05$)

Lastly, a two-way ANOVA was conducted that examined the effect of t_{ct} and F_p on the t_s of a Solar-PV-Wind HRES Grid-tied to an IEEE 14 bus system based on G_s . It was established that there was a statistically significant interaction between the effects of t_{ct} and F_p on the t_s of G_s ($p < 0.05$). This interaction underscores the complex dynamics that dictate G_s stability, influenced by both t_{ct} and F_p level. Similar to the findings for V and f the simple main effects analysis showed that $t_{ct} = 2.00$ s had a significantly higher t_s than $t_{ct} = 1.05$ s

and $t_{ct} = 1.50$ s for all F_p . This consistent trend across all examined parameters suggests that t_{ct} of 2.00 s is particularly detrimental to the system's ability to quickly stabilize, regardless of the F_p level. Moreover, there were statistically significant differences between F_p 1 (0%) and all the other F_p ($p < 0.05$). This finding indicates that any increase in F_p beyond 0% significantly affects the time it takes for G_s to stabilize, further emphasizing the sensitivity of the system's mechanical dynamics to F_p levels.

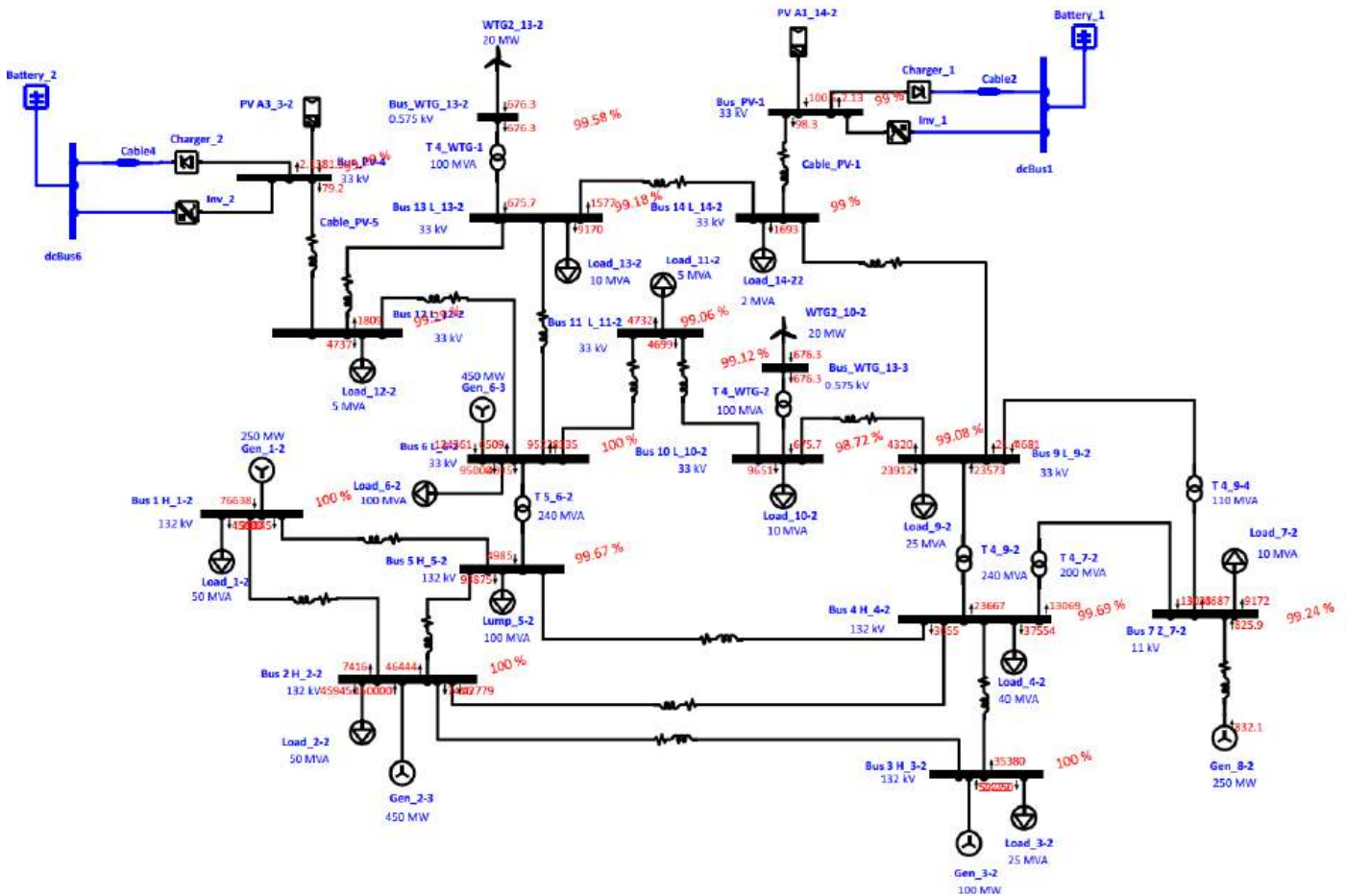


Fig. 9: The simulated Solar PV-Wind-Battery HRES Grid-Tied System and Load Flow Analysis

3.5. Solar PV-Wind-Battery HRES System

For comparative analysis, the Solar PV-Wind-battery system was modeled as the battery was integrated on the Buses with Solar PV, i.e., Bus 12 and 14 as shown in Fig. 9. These Buses were selected because BESS is designed to manage short-term fluctuations in power output from renewable sources and provide support

during disturbances (Ku & Li, 2021). The BESS was modeled with a charger, inverter, and Battery (Table 1).

Similarly, the integration of the HRES into the IEEE 14-bus system significantly altered the power flow across the network. The Solar PV and wind turbines were modeled as distributed generation sources connected to specific buses, while the BESS was also integrated to

manage the variability of renewable generation. The load flow results showed that the power generated by the PV and wind systems was effectively distributed across the buses, reducing the power demand on the conventional generators as shown in Fig.9. Therefore, the BESS played a crucial role in balancing the power flow, particularly during periods of low renewable generation or sudden load changes. Additionally, the voltage profile across the 14 buses was monitored to ensure that all bus voltages remained within acceptable limits (0.97 to 1.00 p.u.).

The simulation results demonstrate the significant role of BESS in enhancing the stability and efficiency of a Solar PV-wind HRES. Specifically, the integration of BESS helps maintain a stable V profile across the network, with V ranging from 0.98772 to 1.000 p.u. This stability is crucial for the reliable operation of the grid, ensuring that voltage levels remain within acceptable limits, which is vital for both the protection of equipment and the consistent delivery of power to end-users (Bignucolo et al., 2017). The observed stability in bus voltages is particularly noteworthy given the inherent variability of RESs such as solar and wind. These sources are often characterized by fluctuations in power generation, which can lead to voltage instability, especially during periods of high load or low generation (Petinrin & Shaabanb, 2016). The minor deviations in V at buses connected to renewable energy sources during these periods underscore the challenges posed by the integration of renewables (Azizipannah-Abarghooee et al., 2024). However, the presence of BESS mitigates

these deviations by providing a buffer that compensates for the variability, thereby maintaining the overall voltage stability of the system (Ehsan & Yang, 2018). Another significant benefit of integrating BESS into the Solar PV-Wind hybrid system is the reduction in line losses. The simulation results indicate an average reduction of 1.25% in line losses compared to the system without BESS. This reduction is attributable to the strategic placement of distributed generation sources close to load centers (Sultana et al., 2016). When power is generated closer to where it is consumed, transmission losses are minimized, thereby enhancing the overall efficiency of the system (Prakash & Khatod, 2016; Sultana et al., 2016). This principle is supported by multiple studies, which have consistently shown that proximity between generation and consumption points leads to lower transmission losses (Abdmouleh et al., 2017; Ehsan & Yang, 2018; Prakash & Khatod, 2016). The BESS further contributes to loss reduction by supplying power locally during peak demand periods (Abdullah et al., 2020). During these times, the electricity demand is high, which can strain the grid and lead to increased losses if power must be transmitted over long distances (Zhou et al., 2021). However, with BESS in place, power can be supplied locally from stored energy, reducing the need to draw power from distant sources (Abdullah et al., 2020). This localized supply not only reduces transmission losses but also eases the burden on the grid during peak periods, contributing to the overall stability and efficiency of the system (Abdullah et al., 2020; Kucevic et al., 2021; Zhou et al., 2021).

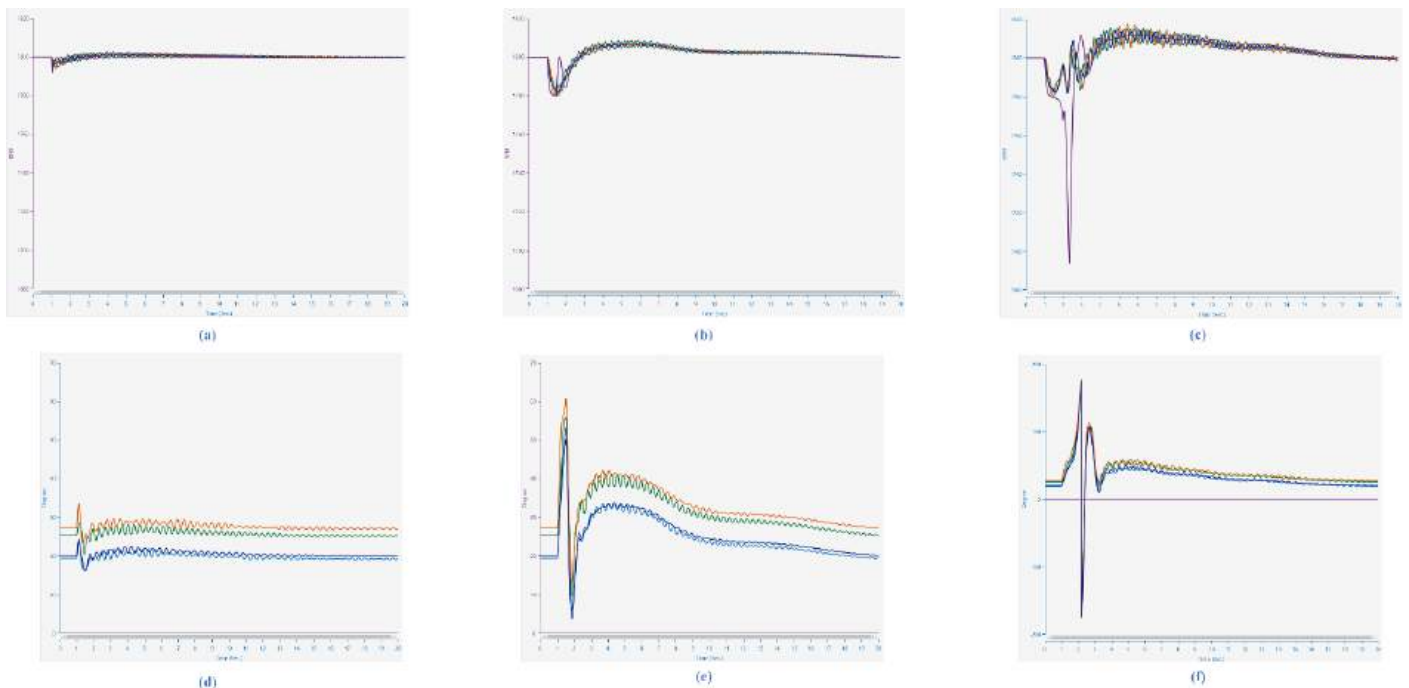


Fig. 10: The plots for Power angle and Speed for the synchronous generators with a fault on Bus 5, (a) Speed at $t_{ct} = 1.05$ s, (b) Speed at $t_{ct} = 1.50$ s, (c) Speed at $t_{ct} = 2.00$ s, (d) Power angle at $t_{ct} = 1.05$ s, (e) Power angle at $t_{ct} = 1.50$ s, (f) Power angle at $t_{ct} = 2.00$ s.

Generally, the integration of BESS into a Solar PV-Wind HRES provides significant benefits in terms of voltage stability and loss reduction. By maintaining stable voltage profiles and reducing line losses, BESS

enhances the reliability and efficiency of the system, making it better suited to accommodate the variable nature of renewable energy sources. These findings align with existing literature, reinforcing the importance of

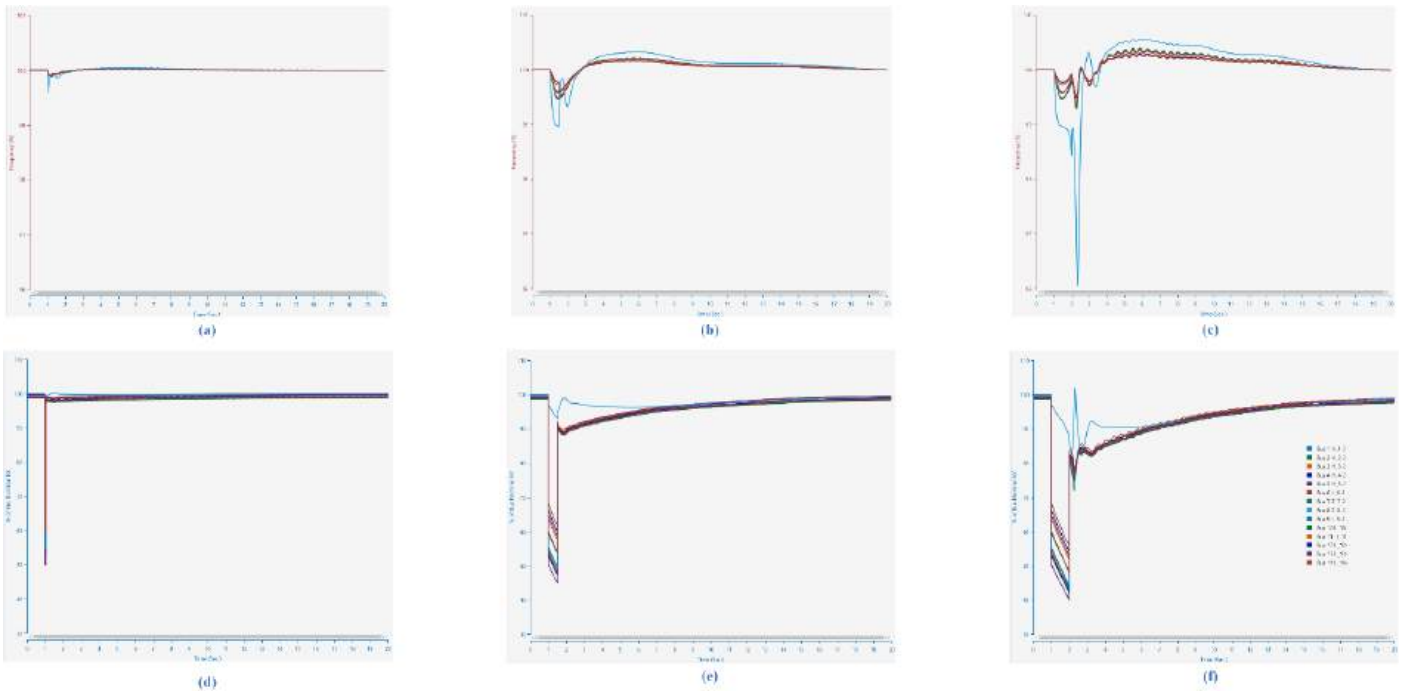


Fig. 11: The plots for Frequency and Voltage for the synchronous generators with a fault on Bus 5, (a) Frequency at $t_{ct} = 1.05\text{ s}$, (b) Frequency at $t_{ct} = 1.50\text{ s}$, (c) Frequency at $t_{ct} = 2.00\text{ s}$, (d) Voltage at $t_{ct} = 1.05\text{ s}$, (e) Voltage at $t_{ct} = 1.50\text{ s}$, (f) Voltage at $t_{ct} = 2.00\text{ s}$.

BESS in modern energy systems, particularly as the share of RESs continues to grow (Hidalgo-León et al., 2017).

3.6. Transient stability analysis

Transient stability analysis was similarly analyzed by simulating sudden disturbances in the system, i.e., LG faults.

3.6.1. Fault on Buses

An LG fault was simulated on all the buses (one at a time) at 1.0 s and the fault was cleared at 1.05 s, 1.5 s, and 2.0 s. From the plots for the power angles and

generator speeds against time in Fig. 10. The results from the study highlight the dynamic behavior of the Solar PV-Wind HRES under fault conditions, with a focus on the V and f responses at different buses. The observed significant oscillations in the system immediately after a fault (oscillations when t_s was larger were greater compared to when t_s is small) are consistent with the findings of Taul et al. (2019), who noted that such oscillations are a common transient response in power systems.

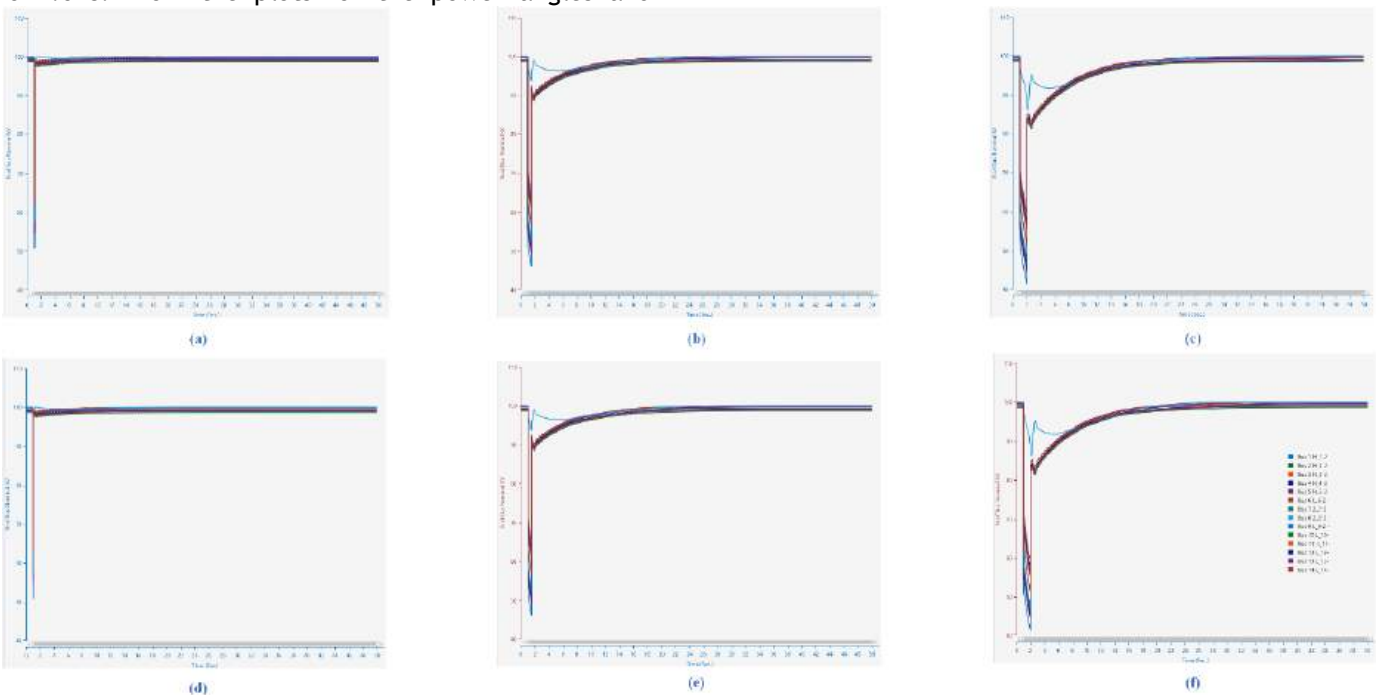


Fig. 12: The differences in the Voltage profile for Solar PV-Wind HRES and Solar PV-Wind-Battery HRES, (a) Solar PV-Wind HRES at $t_{ct} = 1.05\text{ s}$, (b) Solar PV-Wind HRES at $t_{ct} = 1.50\text{ s}$, (c) Solar PV-Wind HRES at $t_{ct} = 2.00\text{ s}$, (d) Solar PV-Wind-Battery HRES at $t_{ct} = 1.05\text{ s}$, (e) Solar PV-Wind-Battery HRES at $t_{ct} = 1.50\text{ s}$, (f) Solar PV-Wind-Battery HRES at $t_{ct} = 2.00\text{ s}$

These oscillations, while inherent in the system's reaction to disturbances, were found to be more pronounced when the t_s was longer. This suggests that the system's ability to stabilize post-fault is contingent on the duration of these oscillations, which can be influenced by various factors, including the system's configuration and the fault clearance time (Awelewa, 2016; Machowski et al., 2020). During the fault, the V and f at the bus where the fault occurred dropped sharply, as expected. This transient response is a typical indication of the system's inability to maintain stability during a fault (Bhui & Senroy, 2016). However, once the fault was cleared, both V and f recovered to their pre-fault levels, as shown in Fig. 11, with the fault at Bus 5. This recovery process is crucial, as it demonstrates the system's resilience and ability to return to steady-state operation after a disturbance (Cassottana et al., 2019). The analysis further revealed that the extent of V and f drops was directly related to the t_{ct} . Faster t_{ct} generally

led to smaller deviations from the nominal values, which underscores the importance of quick fault detection and clearance mechanisms in maintaining system stability.

Moreover, a comparative analysis between Solar PV-Wind HRES and Solar PV-Wind-Battery HRES with a fault at Bus 1 revealed a notable difference in the post-fault behavior. The Solar PV-Wind-Battery HRES system exhibited quicker damping of V oscillations compared to the Solar PV-Wind HRES system, as depicted in Fig. 12. This indicates that the inclusion of a BESS in the hybrid system enhances the system's stability by providing additional support during and after the fault, thus reducing the severity and duration of oscillations (Hasan & Chowdhury, 2023). These results highlight the critical role of t_{ct} and system configuration in determining the stability and resilience of HRES. The inclusion of a BESS in the HRES configuration appears to offer significant advantages in dampening post-fault oscillations, thereby enhancing overall system performance.

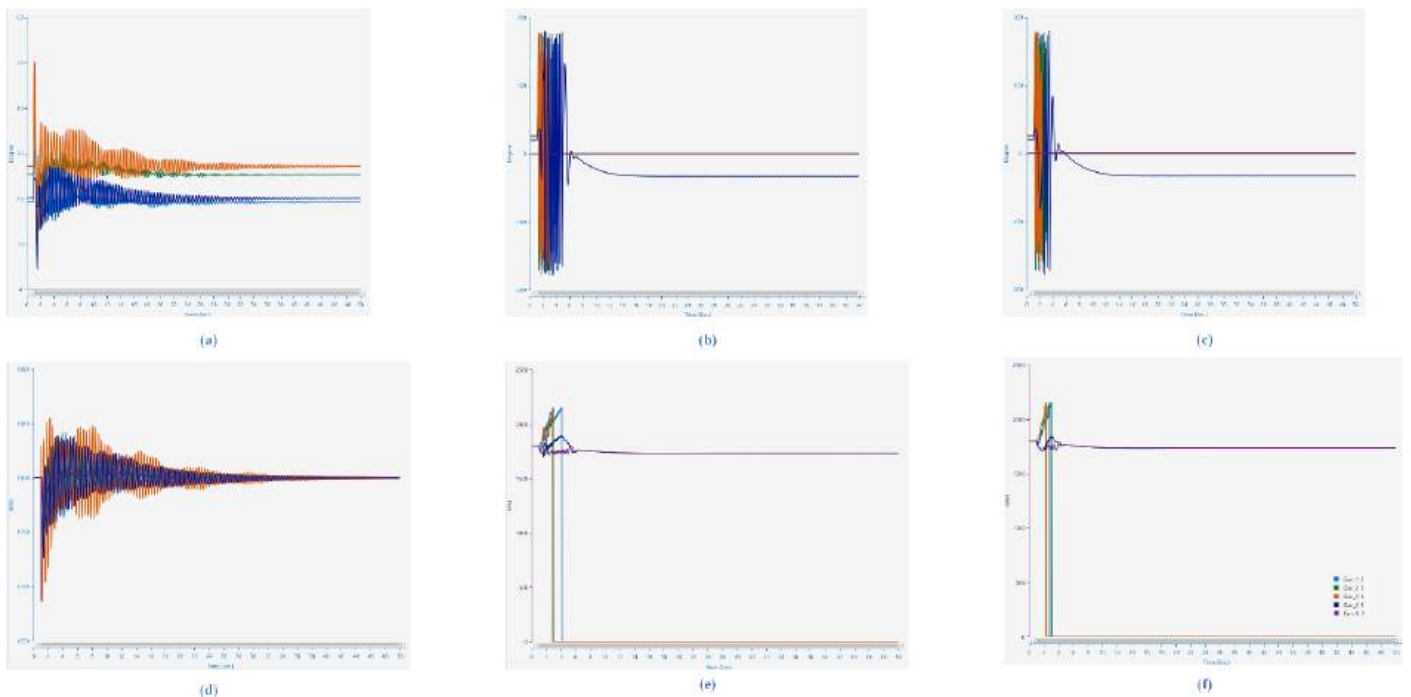


Fig. 13: The plots for the Power angle and Speed for the synchronous generators with a fault on transmission Line 4 at 90% fault position, (a) Power angle at $t_{ct} = 1.05$ s, (b) Power angle at $t_{ct} = 1.50$ s, (c) Power angle at $t_{ct} = 2.00$ s, (d) Speed at $t_{ct} = 1.05$ s, (e) Speed at $t_{ct} = 1.50$ s, (f) Speed at $t_{ct} = 2.00$ s.

3.6.2. Fault on Transmission Lines

Based on a similar analysis as the solar PV-Wind HRES system, Fig. 13 presents the plots for the power angles and generator speeds against time at a F_p of 90% on fault at Line 5. In analyzing the transient stability of a Solar PV-Wind HRES connected to a grid, the study provides crucial insights into the impact of t_{ct} and F_p on system stability. Specifically, the observations at a t_{ct} of 1.05 s indicated that the system's oscillations dampened effectively, leading to stability for the connected generators. This implies that the generators could maintain synchronous operation, recovering from disturbances swiftly without losing synchronization, which is crucial for the continuous operation of the

power system (Cheema, 2020). The dampening of oscillations is indicative of effective fault clearing within a time frame that allows the generators to stabilize (Xiong et al., 2020).

However, when the t_{ct} is extended beyond 1.50 s, the connected generators experience isolation, leading to a shutdown. This indicates that the t_{ct} is a critical parameter in ensuring system stability. If the fault persists too long, it can lead to a situation where the generators can no longer maintain synchronous operation, ultimately leading to their disconnection from the grid (Yaghobi, 2018). This shutdown scenario highlights the importance of prompt fault-clearing mechanisms to prevent widespread instability in the grid

(Mastoi et al., 2023). The study further examines the impact of F_p on system stability, particularly focusing on f and V as key indicators. From the results presented in Fig. 14 and Fig. 15, it is observed that the impact of F_p at 100% is almost identical to that at 0%. This suggests that within the tested range, F_p variations do not

significantly affect system stability. However, the deviation in system response is more pronounced with changes in t_{ct} than with changes in F_p . This highlights that while F_p is a factor in system stability, the timing of fault clearance plays a more crucial role.

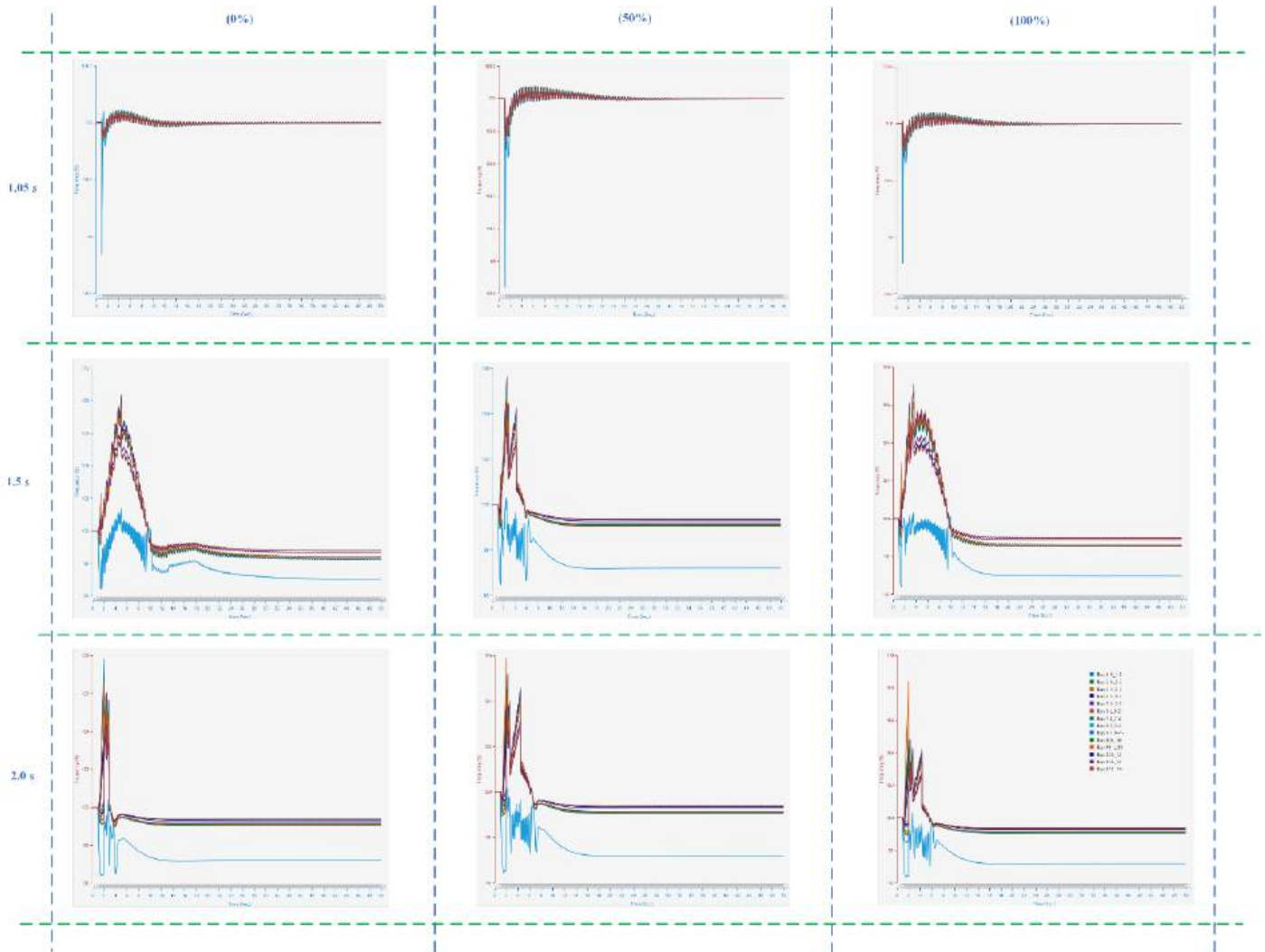


Fig. 14: The plots for Frequency at different F_p and t_{ct}

These findings emphasize the critical role of t_{ct} in maintaining the stability of Solar PV-Wind-Battery HRES connected to the grid. Similarly, the ability of the system to stabilize after a disturbance is highly dependent on how quickly the fault is cleared, with longer delays leading to potential isolation and shutdown of generators. On the other hand, F_p levels, has a less significant impact on the overall system stability, making t_{ct} a more critical parameter to manage for ensuring the reliable operation of grid-tied HRES systems.

3.7. Quantitative analysis

A descriptive statistic of the entire data is given in Table 6 in terms of measures of central tendency and measures of variability (spread) in t_s for G_s , V , and f . It was established that the mean t_s for G_s was 15.513 s with a median of 6.206 s ranging from 1.021 s (minimum) to 50.000 s (maximum). The mean t_s for f was 6.793 s

with a median of 4.691 s ranging from 1.050 s (minimum) to 49.981 s (maximum). Lastly, the mean t_s for V was 14.875 s with a median of 5.781 s ranging from 1.021 s (minimum) to 50.000 s (maximum). Similarly, a Log transformation was performed on the data, and the transformed data normality was ascertained by the Shapiro-Wilk Test.

3.7.1. Fault on buses

For each variable, i.e., f , V , and G_s , the t_s was analyzed as presented in Table 7. Firstly, a two-way ANOVA was conducted that examined the effect of t_{ct} and B on t_s of a Solar-PV-Wind-Battery HRES Grid-tied to an IEEE 14 bus system based on f . There was a statistically significant interaction between the effects of t_{ct} and B on the t_s of f ($p < 0.05$). Indicating that the combined effect of these variables significantly influences the system's t_s after a disturbance, while the

relationship between t_{ct} and the B impact is not straightforward and depends on the interaction between these factors.

However, there was no statistically significant difference in the B on the t_s of f ($p < 0.05$). This indicates that the battery's presence did not independently affect the t_s for frequency, highlighting that other system parameters or the interaction with t_{ct} might play more crucial roles in this context. Additionally, there was a statistically significant

difference in the t_{ct} on the t_s of f ($p < 0.05$), with $t_{ct} = 2.00$ s having a significantly higher t_s than all the other t_{ct} . Similarly, this finding underscores the critical importance of fault clearance time in determining the system's frequency stability. A longer $t_{ct} = 2.00$ s led to a slower return to a steady state, which could imply greater system instability or longer periods of oscillations following a disturbance. This emphasizes the need for rapid fault clearance to enhance system performance.

Table 6: The descriptive statistics of the setting time for generator speed bus frequency and bus voltage ($n = 4060$).

Descriptive statistics	Speed (s)	Frequency (s)	Voltage (s)
Maximum	50.000	49.981	50.000
Minimum	1.021	1.050	1.021
Range	48.979	48.931	48.979
Interquartile Range	19.15	6.72	16.96
Median	6.206	4.691	5.781
Skewness	1.138	3.000	1.291
Mean	15.513	6.793	14.875
Standard error	0.281	0.125	0.268
Standard deviation	17.936	7.962	17.075
Variance	321.716	63.394	291.557

Secondly, a two-way ANOVA was conducted that examined the effect of t_{ct} and B on the t_s of a Solar-PV-Wind HRES Grid-tied to an IEEE 14 bus system based on G_s . There was a statistically significant interaction between the effects of t_{ct} and B on the t_s of G_s ($p < 0.05$). A simple main effects analysis showed that $t_{ct} =$

2.00 s had a significantly higher t_s than $t_{ct} = 1.05$ s and $t_{ct} = 1.50$ s. Furthermore, there were statistically significant differences between $t_{ct} = 1.05$ s and $t_{ct} = 2.00$ s, while there were no statistically significant differences between $t_{ct} = 1.05$ s and $t_{ct} = 1.50$ s.

Table 7: The statistical results of the settling time (t_s) expressed in terms of mean and standard deviation

Fault clearance time (t_{ct})	f (t_s)	V (t_s)	G_s (t_s)
$t_{ct} = 1.05$ s	5.284 ± 0.421	9.568 ± 0.521 ^a	10.129 ± 0.529 ^a
$t_{ct} = 1.50$ s	5.113 ± 0.486	10.045 ± 0.433 ^a	10.991 ± 0.634 ^a
$t_{ct} = 2.00$ s	6.069 ± 0.558	12.921 ± 0.507 ^b	11.621 ± 0.607 ^b

a, b mean ± std within a column with no superscript in common differ significantly ($p < 0.05$)

Lastly, a two-way ANOVA was conducted that examined the effect of t_{ct} and B on the t_s of a Solar-PV-Wind HRES Grid-tied to an IEEE 14 bus system based on V . There was a statistically significant interaction between the effects of t_{ct} and B on the t_s of V ($p < 0.05$). This further reinforces the idea that the combined effects of these variables are crucial in determining the system's dynamic response to faults. A simple main effects analysis showed that $t_{ct} = 2.00$ s had a significantly higher t_s than $t_{ct} = 1.05$ s and $t_{ct} = 1.50$ s. This indicates that longer t_{ct} consistently lead to poorer system performance, not only in terms of f but also V and G_s stability. Additionally, there were statistically significant differences between $t_{ct} = 1.05$ s and $t_{ct} = 2.00$ s, while there were no statistically significant differences between $t_{ct} = 1.05$ s and $t_{ct} = 1.50$ s. This suggests that a t_{ct} of around 1.50 s is an optimal threshold for maintaining both f and V and G_s stability without significantly degrading system performance.

3.7.2. Fault on Transmission Lines

A summary of the data is given in Table 8. It was observed that the t_s for $t_{ct} = 2.00$ s was still much higher than that of $t_{ct} = 1.05$ s and $t_{ct} = 1.50$ s. For each variable, i.e., f , V , and G_s , the t_s was analyzed to determine the effects of t_{ct} , F_p , and B as presented in Table 9. Firstly, a three-way ANOVA was conducted that

examined the effect of t_{ct} , F_p , and B on t_s of a Solar-PV-Wind HRES Grid-tied to an IEEE 14 bus system based on V . There was a statistically significant three-way interaction between t_{ct} , F_p , and B ($p < 0.05$). This implies that the relationship between any two of the variables (t_{ct} , F_p , and B) on the t_s is not consistent across the levels of the third variable. In other words, the influence of t_{ct} on the t_s depends on both the F_p and the presence of a B . This significant interaction indicates that the system's V response is highly sensitive to the specific conditions of t_{ct} , F_p , and B status. It suggests that optimizing these parameters simultaneously is crucial for maintaining voltage stability in the grid-tied system.

Secondly, a three-way ANOVA was conducted that examined the effect of t_{ct} , F_p , and B on t_s of a Solar-PV-Wind HRES Grid-tied to an IEEE 14 bus system based on f . It was established that there was a statistically significant three-way interaction between t_{ct} , F_p , and B ($p < 0.05$). This finding aligns with the results obtained for V , underscoring the complexity of the system's dynamic behavior. The f of the system is a critical parameter in grid stability, and the significant interaction effect suggests that deviations in the t_s of f are influenced by the interaction of t_{ct} , F_p , and the presence of a B .

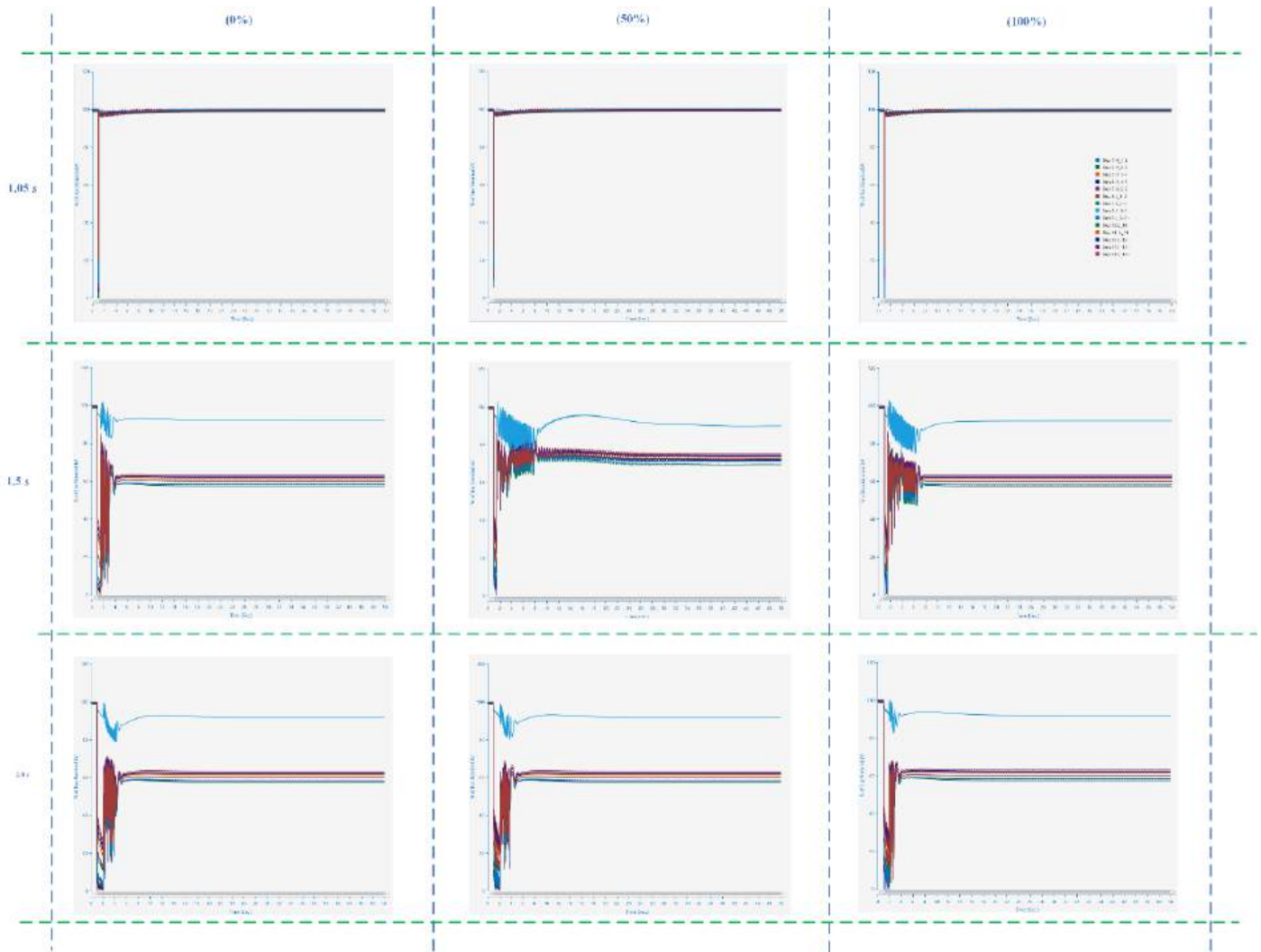


Fig. 15: The plots for Voltage at different F_p and t_{ct} .

Table 8: A summary of the data on the effect of fault position (F_p) and fault clearance time (t_{ct}) on settling time (t_s) for Frequent (f), voltage (V) and generator speed (G_s)

F_p	t_{ct}	$f(t_s)$	$V(t_s)$	$G_s(t_s)$
0% mean \pm std	$t_{ct} = 1.05 s$	2.999 ± 0.357	6.152 ± 0.418	3.529 ± 0.385
	$t_{ct} = 1.50 s$	7.165 ± 0.262	13.728 ± 0.315	7.136 ± 0.304
	$t_{ct} = 2.00 s$	12.565 ± 0.524	23.688 ± 0.397	18.435 ± 0.477
10% mean \pm std	$t_{ct} = 1.05 s$	1.3066 ± 0.104	2.533 ± 0.242	1.453 ± 0.127
	$t_{ct} = 1.50 s$	6.603 ± 0.164	17.090 ± 0.364	11.957 ± 0.385
	$t_{ct} = 2.00 s$	14.668 ± 0.309	34.763 ± 0.425	27.160 ± 0.487
25% mean \pm std	$t_{ct} = 1.05 s$	1.313 ± 0.108	2.545 ± 0.241	1.427 ± 0.122
	$t_{ct} = 1.50 s$	7.964 ± 0.234	15.239 ± 0.349	10.009 ± 0.336
	$t_{ct} = 2.00 s$	15.043 ± 0.369	29.321 ± 0.488	23.963 ± 0.530
50% mean \pm std	$t_{ct} = 1.05 s$	1.376 ± 0.123	2.599 ± 0.246	1.467 ± 0.133
	$t_{ct} = 1.50 s$	6.591 ± 0.149	14.497 ± 0.317	9.548 ± 0.338
	$t_{ct} = 2.00 s$	12.631 ± 0.278	31.580 ± 0.401	24.962 ± 0.503
75% mean \pm std	$t_{ct} = 1.05 s$	1.384 ± 0.117	2.709 ± 0.258	1.496 ± 0.129
	$t_{ct} = 1.50 s$	5.553 ± 0.163	10.551 ± 0.294	6.423 ± 0.232
	$t_{ct} = 2.00 s$	12.328 ± 0.276	28.738 ± 0.398	22.354 ± 0.497
90% mean \pm std	$t_{ct} = 1.05 s$	1.600 ± 0.174	2.965 ± 0.261	1.729 ± 0.175
	$t_{ct} = 1.50 s$	5.697 ± 0.195	10.945 ± 0.356	6.225 ± 0.266
	$t_{ct} = 2.00 s$	8.653 ± 0.200	23.926 ± 0.406	19.434 ± 0.479
100% mean \pm std	$t_{ct} = 1.05 s$	1.223 ± 0.093	3.020 ± 0.289	1.622 ± 0.193
	$t_{ct} = 1.50 s$	7.913 ± 0.246	14.075 ± 0.349	9.822 ± 0.343
	$t_{ct} = 2.00 s$	8.431 ± 0.334	22.970 ± 0.472	16.625 ± 0.527

The significant interaction reveals that these factors cannot be considered in isolation when designing or analyzing the system, as their combined effect can lead

to variations in the system's ability to return to its nominal f after disturbances.

Table 9: The statistical results of the settling time (t_s) expressed in terms of mean and standard deviation

Fault position (F_p)	f (t_s)	V (t_s)	G_s (t_s)
0% mean \pm std	7.576 \pm 0.468 ^a	14.523 \pm 0.492 ^{ae}	9.700 \pm 0.519 ^{ab}
10% mean \pm std	7.526 \pm 0.451 ^{afg}	18.129 \pm 0.566 ^{ad}	13.523 \pm 0.582 ^a
25% mean \pm std	7.937 \pm 0.473 ^{dfg}	15.369 \pm 0.544 ^{aceg}	12.053 \pm 0.556 ^{ab}
50% mean \pm std	6.866 \pm 0.422 ^{achfg}	16.225 \pm 0.532 ^{af}	12.052 \pm 0.558 ^b
75% mean \pm std	6.465 \pm 0.423 ^{aeeg}	14.172 \pm 0.514 ^{efh}	10.091 \pm 0.513 ^b
90% mean \pm std	5.317 \pm 0.359 ^b	12.612 \pm 0.479 ^{ch}	9.129 \pm 0.480 ^b
100% mean \pm std	5.740 \pm 0.429 ^{beh}	13.097 \pm 0.495 ^{bgh}	9.179 \pm 0.508 ^b

a, b mean \pm std within a column with no superscript in common differ significantly ($p < 0.05$)

Lastly, a three-way ANOVA was conducted that examined the effect of t_{ct} , F_p , and B on t_s of a Solar-PV-Wind HRES Grid-tied to an IEEE 14 bus system based on G_s . There was no statistically significant three-way interaction between t_{ct} , F_p , and B ($p < 0.05$). This result indicates that the t_s of G_s is not significantly affected by the combined interaction of t_{ct} , F_p , and B status. This lack of interaction might imply that G_s , unlike V and f , is less sensitive to the simultaneous variations in these parameters or that the system's

design inherently stabilizes generator speed more effectively under varying conditions of t_{ct} , F_p , and B . Therefore, in terms of G_s , the factors may act more independently, with no substantial combined effect on the t_s .

3.7.3. Evaluation of the Effect of Battery Energy Storage System

To evaluate the effect of the Battery on the entire system an independent t-test was performed as given in Table 10.

Table 10: The results for the independent t-test in terms of mean and standard deviation

System	f (mean \pm std)	V (mean \pm std)	G_s (mean \pm std)
PV-Wind	15.843 \pm 0.594 ^a	14.825 \pm 0.524	10.473 \pm 0.543298
PV-Wind Battery	6.781 \pm 0.434 ^b	14.891 \pm 0.519	10.815 \pm 0.532010

a,b mean \pm std within a column, with no superscript in common, differ significantly ($p < 0.05$)

The independent t-test established that there was no statistically significant difference between the PV-Wind Battery Hybrid system and the PV-Wind Hybrid system in terms of t_s of V ($p < 0.05$). Additionally, there was no statistically significant difference between the PV-Wind Battery Hybrid system and the PV-Wind Hybrid system in terms of t_s of G_s ($p < 0.05$). These results indicate that the BESS does not significantly alter the system's V and G_s stability under the conditions tested. These parameters are crucial for maintaining system reliability, and the findings suggest that the hybrid system's overall stability in these aspects is not heavily dependent on the presence of a BESS. However, the PV-Wind Battery Hybrid system had a statistically significantly lower t_s of f compared to the PV-Wind Hybrid system ($p < 0.05$). This highlights the battery's critical role in improving f stability. f stability is vital for the synchronous operation of power systems, and the ability of the BESS to enhance this aspect suggests that it effectively compensates for the inherent variability of renewable energy sources like wind and solar (Datta, 2020). The BESS likely provides rapid frequency support during fluctuations, which is particularly beneficial during events of sudden load changes or renewable output variations (Datta, 2020; Karbouj et al., 2019).

4. Conclusions

The increasing global reliance on renewable energy sources, particularly solar PV and wind energy has necessitated the development of hybrid systems that can harness the strengths of both technologies. Hybrid solar PV-wind grid-tie systems offer a promising solution to the challenges of renewable energy integration, providing enhanced reliability, efficiency, and stability. However, the dynamic nature of these systems, influenced by fluctuating weather conditions and varying

load demands, makes stability analysis a critical area of study. This research focused on the transient stability analysis of a solar PV-wind grid-tie hybrid system, to understand the system's behavior under different operating conditions and identify strategies to enhance its stability based on an IEEE 14 Bus system.

The load flow analysis of the IEEE 14 Bus system established that direct connection between the generator and buses results in higher voltage levels, as there is less impedance and fewer losses between the generator and these buses. The bus voltages ranged from 0.9832 p.u. to 1.00 p.u. Additionally, the Load Flow analysis aimed to identify the optimal buses for the integration of Solar PV and Wind resources by focusing on those that are furthest from the generator yet exhibit stable voltage profiles. This strategy is beneficial as it supports the distributed generation model, enhances voltage stability, reduces transmission losses, and improves overall grid efficiency. Therefore, by carefully selecting the buses for renewable integration, the power system can accommodate clean energy sources while maintaining stability and reliability, which are crucial for the sustainable development of the grid.

On the analysis of transient stability of the hybrid grid-tie system under sudden changes, i.e., faults on transmission lines and buses. The integration of PV and wind systems into the IEEE 14-bus system does result in some variations in voltage and changes in power flow patterns, i.e., 0.9929 p.u. to 0.99 p.u. for buses connected to the PV system and 0.9878 p.u. to 0.9918 p.u. for buses connected to the wind system. Therefore, these changes are manageable and do not compromise the overall stability of the system. Additionally, the integration of renewable energy sources into the power

grid does introduce additional reactive power flows leading to a slight increase in system losses (about 0.02%), the impact is minimal and does not significantly affect system efficiency. When the fault occurred on the buses both voltage, frequency, and generator speed experienced a significant drop but showed a notable recovery to pre-fault levels once the fault was cleared. However, the level of V and f drops were directly proportional to t_{ct} . However, when the fault occurs on the transmission line as the fault clearance time increases (greater than 1.05 s) the generators connected to the faulted line will be isolated. Additionally, fault position doesn't have much effect on the voltage and frequency profiles, however, the fault clearance time had a noticeable effect. i.e., the settling time for the fault clearance time of 1.50 s and 2.00 s were longer compared to those of 1.05 s. Moreover, in the analysis of t_{ct} and t_s for V , f , and G_s , shorter t_{ct} values consistently led to faster stabilization times, which is advantageous for maintaining system stability during transient disturbances. The integration of BESS into a Solar PV-Wind hybrid energy system provided significant benefits in terms of voltage stability (0.98772 to 1.000 p.u.) and loss reduction (1.25%). The BESS enhances the reliability and efficiency of the system by maintaining stable voltage profiles and reducing line losses, making it better suited to accommodate the variable nature of RESs.

References

- Abdi, H., Beigvand, S. D., & La Scala, M. (2017). A review of optimal power flow studies applied to smart grids and microgrids. *Renewable and Sustainable Energy Reviews*, 71, 742-766.
- Abdmouleh, Z., Gastli, A., Ben-Brahim, L., Haouari, M., & Al-Emadi, N. A. (2017). Review of optimization techniques applied for the integration of distributed generation from renewable energy sources. *Renewable Energy*, 113, 266-280.
- Abdullah, W. S. W., Osman, M., Ab Kadir, M. Z. A., & Verayiah, R. (2020). Battery energy storage system (BESS) design for peak demand reduction, energy arbitrage and grid ancillary services. *Int J Pow Elec & Dri Syst ISSN*, 2088(8694), 8694.
- Ahmed, M. M. R., Mirsaedi, S., Koondhar, M. A., Karami, N., Tag-Eldin, E. M., Ghamry, N. A., El-Sehiemy, R. A., Alaas, Z. M., Mahariq, I., & Sharaf, A. M. (2024). Mitigating Uncertainty Problems of Renewable Energy Resources Through Efficient Integration of Hybrid Solar PV/Wind Systems Into Power Networks. *IEEE Access*, 12, 30311-30328.
- Ahmed, S. D., Al-Ismael, F. S. M., Shafiullah, M., Al-Sulaiman, F. A., & El-Amin, I. M. (2020). Grid integration challenges of wind energy: A review. *Ieee Access*, 8, 10857-10878.
- Akram, S., & Ann, Q. U. (2015). Newton raphson method. *International Journal of Scientific & Engineering Research*, 6(7), 1748-1752.
- Alam, M. S., Al-Ismael, F. S., Salem, A., & Abido, M. A. (2020). High-level penetration of renewable energy sources into grid utility: Challenges and solutions. *IEEE Access*, 8, 190277-190299.
- Alnawafah, H. (2024). *Modeling and integration of smart control strategies to improve large-scale pv system management and operation in a low inertia power grid*.
- Alsakati, A. A., Vaithilingam, C. A., & Alnasseir, J. (2021). Transient stability assessment of IEEE 9-bus system integrated wind farm. *MATEC Web of Conferences*, 335, 2006.
- Amran, M. E., & Muhtazaruddin, M. N. (2019). Renewable energy optimization review: variables towards competitive advantage in green building development. *Progress in Energy and Environment*, 1-15.
- Auer, S., Hellmann, F., Krause, M., & Kurths, J. (2017). Stability of synchrony against local intermittent fluctuations in tree-like power grids. *Chaos: An Interdisciplinary Journal of Nonlinear Science*, 27(12).
- Awelewa, A. A. (2016). Development of Nonlinear Control Schemes for Electric Power System Stabilization. *Phd. Diss, Covenant University*
- Azizipanah-Abarghooee, R., Malekpour, M., Karimi, M., & Terzija, V. (2024). Integration of wind and solar energies with battery energy storage systems into 36-zone Great Britain power system for frequency regulation studies. *International Journal of Electrical Power & Energy Systems*, 156, 109737.
- Babatunde, O. M., Munda, J. L., & Hamam, Y. (2020). A comprehensive state-of-the-art survey on hybrid renewable energy system operations and planning. *IEEE Access*, 8, 75313-75346.
- Babu, T. S., Vasudevan, K. R., Ramachandaramurthy, V. K., Sani, S. B., Chemud, S., & Lajim, R. M. (2020). A comprehensive review of hybrid energy storage systems: Converter topologies, control strategies and future prospects. *IEEE Access*, 8, 148702-148721.
- Basit, M. A., Dilshad, S., Badar, R., & Sami ur Rehman, S. M. (2020). Limitations, challenges, and solution approaches in grid-connected renewable energy systems. *International Journal of Energy Research*, 44(6), 4132-4162.
- Benali, A., Khiat, M., Allaoui, T., & Denai, M. (2018). Power quality improvement and low voltage ride through capability in hybrid wind-PV farms grid-connected using dynamic voltage restorer. *IEEE Access*, 6, 68634-68648.
- Bessa, R., Moreira, C., Silva, B., & Matos, M. (2019). Handling renewable energy variability and uncertainty in power system operation. *Advances in Energy Systems: The Large-scale Renewable Energy Integration Challenge*, 1-26.
- Bignucolo, F., Cerretti, A., Coppo, M., Savio, A., & Turri, R. (2017). Effects of energy storage systems grid code requirements on interface protection performances in low voltage networks. *Energies*, 10(3), 387.
- Blaabjerg, F., Yang, Y., Yang, D., & Wang, X. (2017). Distributed power-generation systems and protection. *Proceedings of the IEEE*, 105(7), 1311-1331.

- Bossanyi, E. A. (2003). Wind turbine control for load reduction. *Wind Energy: An International Journal for Progress and Applications in Wind Power Conversion Technology*, 6(3), 229-244.
- Cassottana, B., Shen, L., & Tang, L. C. (2019). Modeling the recovery process: A key dimension of resilience. *Reliability Engineering & System Safety*, 190, 106528.
- Cheema, K. M. (2020). A comprehensive review of virtual synchronous generator. *International Journal of Electrical Power & Energy Systems*, 120, 106006.
- Celik, A. N. (2021). Analysis of Energy Supply, Installed Power and Renewable Capacity in the World, the EU and Turkey. *Düzce Üniversitesi Bilim ve Teknoloji Dergisi*, 9(3), 500-519.
- Chen, K., Huang, C., & He, J. (2016). Fault detection, classification and location for transmission lines and distribution systems: a review on the methods. *High Voltage*, 1(1), 25-33.
- Chen, Y. Q., Fink, O., & Sansavini, G. (2017). Combined fault location and classification for power transmission lines fault diagnosis with integrated feature extraction. *IEEE Transactions on Industrial Electronics*, 65(1), 561-569.
- Cifuentes, N., Rahmann, C., Valencia, F., & Alvarez, R. (2019). Network allocation of BESS with voltage support capability for improving the stability of power systems. *IET Generation, Transmission & Distribution*, 13(6), 939-949.
- Corneo, G., & Jeanne, O. (2009). A theory of tolerance. *Journal of Public Economics*, 93(5-6), 691-702.
- Das, C. K., Bass, O., Kothapalli, G., Mahmoud, T. S., & Habibi, D. (2018). Overview of energy storage systems in distribution networks: Placement, sizing, operation, and power quality. *Renewable and Sustainable Energy Reviews*, 91, 1205-1230.
- Datta, S., Chattopadhyaya, A., Chattopadhyay, S., & Das, A. (2020). Line to ground and line to line fault analysis in IEEE standard 9 BUS system. *Journal Homepage: Http://lieta.Org/Journals/Mmc_a*, 93(1-4), 10-18.
- De Winter, J. C. F. (2019). Using the Student's t-test with extremely small sample sizes. *Practical Assessment, Research, and Evaluation*, 18(1), 10.
- Do Coutto Filho, M. B., de Souza, J. S., Glover, J. D., Flôr, V. B., Nishio, A., Lima, R., Daibes, J. V., Quintanilha, L., Coimbra, A., & Soares, W. (2022). Educational Tool for Power System State Estimation Teaching and Learning. *IEEE Transactions on Power Systems*, 38(6), 5885-5895.
- Ehsan, A., & Yang, Q. (2018). Optimal integration and planning of renewable distributed generation in the power distribution networks: A review of analytical techniques. *Applied Energy*, 210, 44-59.
- Emad, D., El-Hameed, M. A., Yousef, M. T., & El-Fergany, A. A. (2020). Computational methods for optimal planning of hybrid renewable microgrids: a comprehensive review and challenges. *Archives of Computational Methods in Engineering*, 27, 1297-1319.
- Farrokhabadi, M., König, S., Cañizares, C. A., Bhattacharya, K., & Leibfried, T. (2017). Battery energy storage system models for microgrid stability analysis and dynamic simulation. *IEEE Transactions on Power Systems*, 33(2), 2301-2312.
- Flynn, D., Rather, Z., Árdal, A. R., D'Arco, S., Hansen, A. D., Cutululis, N. A., Sorensen, P., Estanqueiro, A., Gómez-Lázaro, E., & Menemenlis, N. (2019). Technical impacts of high penetration levels of wind power on power system stability. *Advances in Energy Systems: The Large-scale Renewable Energy Integration Challenge*, 47-65.
- Gholami, A., Shekari, T., Amirioun, M. H., Aminifar, F., Amini, M. H., & Sargolzaei, A. (2018). Toward a consensus on the definition and taxonomy of power system resilience. *IEEE Access*, 6, 32035-32053.
- González-Estrada, E., Villaseñor, J. A., & Acosta-Pech, R. (2022). Shapiro-Wilk test for multivariate skew-normality. *Computational Statistics*, 37(4), 1985-2001.
- Guo, H., Zheng, C., Lu, H. H.-C., & Fernando, T. (2017). A critical review of cascading failure analysis and modeling of power system. *Renewable and Sustainable Energy Reviews*, 80, 9-22.
- Hamzeh, A., Hamed, S. A., & Al-Omari, Z. (2018). Wind Generation Impact on Symmetrical Fault Level at Grid Buses. *International Journal of Electrical & Computer Engineering (2088-8708)*, 8(5).
- Hasheminamin, M., Agelidis, V. G., Ahmadi, A., Siano, P., & Teodorescu, R. (2018). Single-point reactive power control method on voltage rise mitigation in residential networks with high PV penetration. *Renewable Energy*, 119, 504-512.
- Hashim, N., Hamzah, N., Latip, M. F. A., & Sallehuddin, A. A. (2012). Transient stability analysis of the IEEE 14-bus test system using dynamic computation for power systems (DCPS). *2012 Third International Conference on Intelligent Systems Modelling and Simulation*, 481-486.
- Hassan, Q., Viktor, P., Al-Musawi, T. J., Ali, B. M., Algburi, S., Alzoubi, H. M., Al-Jiboory, A. K., Sameen, A. Z., Salman, H. M., & Jaszczur, M. (2024). The renewable energy role in the global energy Transformations. *Renewable Energy Focus*, 48, 100545.
- He, X., Geng, H., Li, R., & Pal, B. C. (2019). Transient stability analysis and enhancement of renewable energy conversion system during LVRT. *IEEE Transactions on Sustainable Energy*, 11(3), 1612-1623.
- Hidalgo-León, R., Siguenza, D., Sanchez, C., León, J., Jácome-Ruiz, P., Wu, J., & Ortiz, D. (2017). A survey of battery energy storage system (BESS), applications and environmental impacts in power systems. *2017 Ieee Second Ecuador Technical Chapters Meeting (EtcM)*, 1-6.
- Hosseinzadeh, N., Aziz, A., Mahmud, A., Gargoom, A., & Rabbani, M. (2021). Voltage stability of power systems with renewable-energy inverter-based generators: A review. *Electronics*, 10(2), 115.
- IPCC. (2018). Global warming of 1.5° C. Summary for

- Policymakers. In *Contribution of Working Groups I, II and III to the 48th Session of the IPCC*. Republic of Korea Incheon.
- IRENA. (2020). *Renewable Power Generation Costs in 2019*. <https://www.irena.org/publications/2020/Jun/Renewable-Power-Costs-in-2019>
- Ismail, B., Wahab, N. I. A., Othman, M. L., Radzi, M. A. M., Vijayakumar, K. N., & Naain, M. N. M. (2020). A comprehensive review on optimal location and sizing of reactive power compensation using hybrid-based approaches for power loss reduction, voltage stability improvement, voltage profile enhancement and loadability enhancement. *IEEE Access*, 8, 222733-222765.
- Iyambo, P. K., & Tzoneva, R. (2007). Transient stability analysis of the IEEE 14-bus electric power system. *AFRICON 2007*, 1-9.
- James, J. Q., Hill, D. J., Lam, A. Y. S., Gu, J., & Li, V. O. K. (2017). Intelligent time-adaptive transient stability assessment system. *IEEE Transactions on Power Systems*, 33(1), 1049-1058.
- Kabeyi, M. J. B., & Olanrewaju, O. A. (2022). Sustainable energy transition for renewable and low carbon grid electricity generation and supply. *Frontiers in Energy Research*, 9.
- Khadka, N., Paudel, R., Adhikary, B., Bista, A., Sharma, S., & Shrestha, A. (2020). Transient stability in renewable energy penetrated power systems: A review. *Proceedings of the RESSD 2020 International Conference on Role of Energy for Sustainable Social Development in 'New Normal' Era, Kathmandu, Nepal*, 28-29.
- Kow, K. W., Wong, Y. W., Rajkumar, R. K., & Rajkumar, R. K. (2016). A review on performance of artificial intelligence and conventional method in mitigating PV grid-tied related power quality events. *Renewable and Sustainable Energy Reviews*, 56, 334-346.
- Ku, T.-T., & Li, C.-S. (2021). Implementation of battery energy storage system for an island microgrid with high PV penetration. *IEEE Transactions on Industry Applications*, 57(4), 3416-3424.
- Kucevic, D., Semmelmann, L., Collath, N., Jossen, A., & Hesse, H. (2021). Peak shaving with battery energy storage systems in distribution grids: a novel approach to reduce local and global peak loads. *Electricity*, 2(4), 573-589.
- Kumar, S., Kumar, A., & Sharma, N. K. (2020). A novel method to investigate voltage stability of IEEE-14 bus wind integrated system using PSAT. *Frontiers in Energy*, 14(2), 410-418.
- Lee, D. K. (2020). Data transformation: a focus on the interpretation. *Korean Journal of Anesthesiology*, 73(6), 503-508.
- Li, C., Chaudhary, S. K., Savaghebi, M., Vasquez, J. C., & Guerrero, J. M. (2016). Power flow analysis for low-voltage AC and DC microgrids considering droop control and virtual impedance. *IEEE Transactions on Smart Grid*, 8(6), 2754-2764.
- Maaruf, M., Khan, K., & Khalid, M. (2022). Robust control for optimized islanded and grid-connected operation of solar/wind/battery hybrid energy. *Sustainability*, 14(9), 5673.
- Machowski, J., Lubosny, Z., Bialek, J. W., & Bumby, J. R. (2020). *Power system dynamics: stability and control*. John Wiley & Sons.
- Medina, C., Ana, C. R. M., & González, G. (2022). Transmission grids to foster high penetration of large-scale variable renewable energy sources-A review of challenges, problems, and solutions. *International Journal of Renewable Energy Research (IJRER)*, 12(1), 146-169.
- Meegahapola, L. G., Bu, S., Wadduwage, D. P., Chung, C. Y., & Yu, X. (2020). Review on oscillatory stability in power grids with renewable energy sources: Monitoring, analysis, and control using synchrophasor technology. *IEEE Transactions on Industrial Electronics*, 68(1), 519-531.
- Mehra, M. K., Mukherjee, S., Bhattacharya, G., & Azharuddin, S. M. (2021). Renewable Energy in India: What It Means for the Economy and Jobs. *Sustainable Development Insights from India: Selected Essays in Honour of Ramprasad Sengupta*, 343-375.
- Mlilo, N., Brown, J., & Ahfock, T. (2021). Impact of intermittent renewable energy generation penetration on the power system networks-A review. *Technology and Economics of Smart Grids and Sustainable Energy*, 6(1), 25.
- Mojallal, A., & Lotfifard, S. (2017). Enhancement of grid connected PV arrays fault ride through and post fault recovery performance. *IEEE Transactions on Smart Grid*, 10(1), 546-555.
- Morshed, M. J., & Fekih, A. (2019). A novel fault ride through scheme for hybrid wind/PV power generation systems. *IEEE Transactions on Sustainable Energy*, 11(4), 2427-2436.
- Nagpal, M., & Henville, C. (2017). Impact of power-electronic sources on transmission line ground fault protection. *IEEE Transactions on Power Delivery*, 33(1), 62-70.
- Newell, R., Raimi, D., Villanueva, S., & Prest, B. (2021). Global energy outlook 2021: pathways from Paris. *Resources for the Future*, 8, 39.
- Nikolaev, N., Dimitrov, K., & Rangelov, Y. (2021). A comprehensive review of small-signal stability and power oscillation damping through photovoltaic inverters. *Energies*, 14(21), 7372.
- Nsaif, Y. M., Lipu, M. S. H., Ayob, A., Yusof, Y., & Hussain, A. (2021). Fault detection and protection schemes for distributed generation integrated to distribution network: Challenges and suggestions. *IEEE Access*, 9, 142693-142717.
- Østergaard, P. A., Duic, N., Noorollahi, Y., Mikulcic, H., & Kalogirou, S. (2020). Sustainable development using renewable energy technology. In *Renewable energy* (Vol. 146, pp. 2430-2437). Elsevier.
- Ourahou, M., Ayrir, W., Hassouni, B. E. L., & Haddi, A. (2020). Review on smart grid control and reliability in presence of renewable energies: Challenges and

- prospects. *Mathematics and Computers in Simulation*, 167, 19-31.
- Owais, R., & Iqbal, S. J. (2023). An intelligent two-level control of solar photovoltaic power plant for electromechanical oscillation damping in power systems. *Arabian Journal for Science and Engineering*, 48(5), 6271-6292.
- Panda, D. K., & Das, S. (2021). Smart grid architecture model for control, optimization and data analytics of future power networks with more renewable energy. *Journal of Cleaner Production*, 301, 126877.
- Petinrin, J. O., & Shaabanb, M. (2016). Impact of renewable generation on voltage control in distribution systems. *Renewable and Sustainable Energy Reviews*, 65, 770-783.
- Pfeifer, A., Dobravec, V., Pavlinek, L., Krajačić, G., & Duić, N. (2018). Integration of renewable energy and demand response technologies in interconnected energy systems. *Energy*, 161, 447-455. <https://doi.org/10.1016/j.energy.2018.07.134>
- Potrc, S., Čuček, L., Martin, M., & Kravanja, Z. (2021). Sustainable renewable energy supply networks optimization-The gradual transition to a renewable energy system within the European Union by 2050. *Renewable and Sustainable Energy Reviews*, 146, 111186.
- Prakash, P., & Khatod, D. K. (2016). Optimal sizing and siting techniques for distributed generation in distribution systems: A review. *Renewable and Sustainable Energy Reviews*, 57, 111-130.
- Reddy, M. V., Muni, B. P., & Sarma, A. (2016). Enhancement of voltage profile for IEEE 14 bus system with inter line power flow controller. *2016 Biennial International Conference on Power and Energy Systems: Towards Sustainable Energy (PESTSE)*, 1-5.
- Reddy, S. S. (2017). Optimal power flow with renewable energy resources including storage. *Electrical Engineering*, 99, 685-695.
- Reza, M. S., Hannan, M. A., Ker, P. J., Mansor, M., Lipu, M. S. H., Hossain, M. J., & Mahlia, T. M. I. (2023). Uncertainty parameters of battery energy storage integrated grid and their modeling approaches: A review and future research directions. *Journal of Energy Storage*, 68, 107698.
- Rousselet, G. A., & Wilcox, R. R. (2018). Reaction times and other skewed distributions: problems with the mean and the median. *BioRxiv*, 383935.
- Roy, P., He, J., Zhao, T., & Singh, Y. V. (2022). Recent advances of wind-solar hybrid renewable energy systems for power generation: A review. *IEEE Open Journal of the Industrial Electronics Society*, 3, 81-104.
- Samakpong, T., Ongsakul, W., & Madhu Manjiparambil, N. (2022). Optimal power flow incorporating renewable uncertainty related opportunity costs. *Computational Intelligence*, 38(3), 1057-1082.
- Sarkar, M. N. I., Meegahapola, L. G., & Datta, M. (2018). Reactive power management in renewable rich power grids: A review of grid-codes, renewable generators, support devices, control strategies and optimization algorithms. *Ieee Access*, 6, 41458-41489.
- Shair, J., Li, H., Hu, J., & Xie, X. (2021). Power system stability issues, classifications and research prospects in the context of high-penetration of renewables and power electronics. *Renewable and Sustainable Energy Reviews*, 145, 111111.
- Shakerighadi, B., Johansson, N., Eriksson, R., Mitra, P., Bolzoni, A., Clark, A., & Nee, H. (2023). An overview of stability challenges for power-electronic-dominated power systems: The grid-forming approach. *IET Generation, Transmission & Distribution*, 17(2), 284-306.
- Shapiro, S. S., & Wilk, M. B. (1965). An analysis of variance test for normality (complete samples). *Biometrika*, 52(3-4), 591-611.
- Sharafutdinov, K., Rydin Gorjão, L., Matthiae, M., Faulwasser, T., & Witthaut, D. (2018). Rotor-angle versus voltage instability in the third-order model for synchronous generators. *Chaos: An Interdisciplinary Journal of Nonlinear Science*, 28(3).
- Shivashankar, S., Mekhilef, S., Mokhlis, H., & Karimi, M. (2016). Mitigating methods of power fluctuation of photovoltaic (PV) sources-A review. *Renewable and Sustainable Energy Reviews*, 59, 1170-1184.
- Sinsel, S. R., Riemke, R. L., & Hoffmann, V. H. (2020). Challenges and solution technologies for the integration of variable renewable energy sources—a review. *Renewable Energy*, 145, 2271-2285.
- Siva, A. S., Sathieshkumar, S., & Kumar, T. S. (2020). Analysis of stability in IEEE 14 bus system using ETAP Software. *2020 Fourth International Conference on Inventive Systems and Control (ICISC)*, 935-938.
- Somerfield, P. J., Clarke, K. R., & Gorley, R. N. (2021a). Analysis of similarities (ANOSIM) for 2-way layouts using a generalised ANOSIM statistic, with comparative notes on Permutational Multivariate Analysis of Variance (PERMANOVA). *Austral Ecology*, 46(6), 911-926.
- Somerfield, P. J., Clarke, K. R., & Gorley, R. N. (2021b). Analysis of similarities (ANOSIM) for 3-way designs. *Austral Ecology*, 46(6), 927-941.
- Stanelytė, D., & Radziukynas, V. (2022). Analysis of voltage and reactive power algorithms in low voltage networks. *Energies*, 15(5), 1843.
- Sultana, U., Khairuddin, A. B., Aman, M. M., Mokhtar, A. S., & Zareen, N. (2016). A review of optimum DG placement based on minimization of power losses and voltage stability enhancement of distribution system. *Renewable and Sustainable Energy Reviews*, 63, 363-378.
- Taul, M. G., Wang, X., Davari, P., & Blaabjerg, F. (2019). An overview of assessment methods for synchronization stability of grid-connected converters under severe symmetrical grid faults. *IEEE Transactions on Power Electronics*, 34(10), 9655-9670.
- Venkatesan, R., Kumar, C., Balamurugan, C. R., & Senjyu,

- T. (2024). Enhancing power quality in grid-connected hybrid renewable energy systems using UPQC and optimized O-FOPID. *Frontiers in Energy Research*, 12, 1425412.
- Wang, Y., Ravishankar, J., & Phung, T. (2016). A study on critical clearing time (CCT) of micro-grids under fault conditions. *Renewable Energy*, 95, 381-395.
- Xiong, X., Wu, C., Hu, B., Pan, D., & Blaabjerg, F. (2020). Transient damping method for improving the synchronization stability of virtual synchronous generators. *IEEE Transactions on Power Electronics*, 36(7), 7820-7831.
- Xu, B., Chen, D., Venkateshkumar, M., Xiao, Y., Yue, Y., Xing, Y., & Li, P. (2019). Modeling a pumped storage hydropower integrated to a hybrid power system with solar-wind power and its stability analysis. *Applied Energy*, 248, 446-462.
- Yaghoobi, H. (2018). Fast predictive technique for reverse power detection in synchronous generator. *IET Electric Power Applications*, 12(4), 508-517.
- Yang, D., Wang, X., Liu, F., Xin, K., Liu, Y., & Blaabjerg, F. (2017). Adaptive reactive power control of PV power plants for improved power transfer capability under ultra-weak grid conditions. *IEEE Transactions on Smart Grid*, 10(2), 1269-1279.
- Ye, H., Liu, Y., Zhang, P., & Du, Z. (2016). Analysis and detection of forced oscillation in power system. *IEEE Transactions on Power Systems*, 32(2), 1149-1160.
- Yousefian, R., Bhattarai, R., & Kamalasadani, S. (2017). Transient stability enhancement of power grid with integrated wide area control of wind farms and synchronous generators. *IEEE Transactions on Power Systems*, 32(6), 4818-4831.
- Yu, D. J., Schoon, M. L., Hawes, J. K., Lee, S., Park, J., Rao, P. S. C., Siebeneck, L. K., & Ukkusuri, S. V. (2020). Toward general principles for resilience engineering. *Risk Analysis*, 40(8), 1509-1537.
- Zhou, H. S., Passey, R., Bruce, A., & Sproul, A. B. (2021). Aggregated impact of coordinated commercial-scale battery energy storage systems on network peak demand, and financial outcomes. *Renewable and Sustainable Energy Reviews*, 144, 111014.